dCollection

Doctoral Dissertation

Avenanthramide-C Rescues Ototoxicity Induced by Anti-cancer Drugs: Methotrexate or Cisplatin

Graduate School of Medicine, Chonnam National University

Department of Biomedical Sciences

Alphonse Umugire

February 2023

Avenanthramide-C Rescues Ototoxicity Induced by Anti-cancer Drugs: Methotrexate or Cisplatin

Department of Biomedical Sciences

Graduate School of Medicine, Chonnam National University

Alphonse Umugire

Supervised by **Professor Hyong-Ho Cho**

A dissertation submitted in partial fulfillment of the requirements for the **Doctor of Philosophy in Biomedical Sciences.**

Committee in Charge:

Han-Seong Jeong

Sungsu Lee

Byeong Chae Kim

Sujeong Jang

Hyong-Ho Cho

February 2023

Contents

LIST OF ABBREVIATIONS

1. ABR = Auditory brainstem response

2. ATP = Adenosine triphosphate

3. AVN-C = Avenanthramide-C

4. BAX = BCL2 Associated X

5. BLB = Blood labyrinthine barrier

6. Ca = Calcium

7. CBD = Calbindin

8. COX2 = Cyclooxygenase 2

9. CP = Cisplatin

10. CtBP2 = C-terminal binding protein

11. dB = Decibel

12. DCF = 2', 7' –Dichlorofluorescein

13. DIHL = Drug-induced hearing loss

14. DMSO = Dimethyl sulfoxide

15. DNA = Deoxyribonucleic acid

16. EDTA = Ethylenediaminetetraacetic acid

17. FA = Folinic Acid

18. GM = Gentamicin

19. HD-MTX = High-dose methotrexate

20. HEI-OC1 = House Ear Institute-Organ of Corti1

21. HL = Hearing loss

22. HRK = Harakiri, BCL2 Interacting Protein

23. IHCs = Inner hair cells

24. IL1β = Interleukin-1-beta

25. IL6 = Interleukin-6

26. iNOS = Inducible nitric oxide synthase

27. IP = Intraperitoneal

28. IV = Intravenous

29. KO = Knockout

30. LC-MS = Liquid Chromatography-Mass Spectrophotometry

31. MTT = Thiazolyl Blue Tetrazolium Bromide

32. MTX = Methotrexate

33. Myo7a = Myosin-7a

34. NF200 = Anti-Neurofilament 200

35. NIHL = Noise-induced hearing loss

36. NO = Nitric oxide

37. OC = Organ of Corti

38. OHCs = Outer Hair Cells

39. PBS = Phosphate-Buffered Saline

40. PFA = Paraformaldehyde

41. PL = Phalloidin

42. Pres = Presitin

43. PT = Permanent Threshold

44. PTS = Permanent threshold shift

45. RNA = Ribonucleic acid

46. RNS = Reactive nitrogen species

47. ROS = Reactive oxygen species

48. RT = Room Temperature

49. RT-PCR = Reverse transcription polymerase chain reaction

50. SD = Standard deviation

51. SGNs = Spiral ganglion neurons

52. SPL = Sound pressure level

53. TNFα = Tumor necrosis factor alpha

54. TTS = Transient threshold shift

55. WHO = World Health Organization

56. WT = Wild type

LIST OF FIGURES

LIST OF TABLES

x

Avenanthramide-C Rescues Ototoxicity Induced by Anti-cancer Drugs: Methotrexate or Cisplatin

ABSTRACT

Introduction. Chemotherapy medicines like methotrexate (MTX) and cisplatin (CP) are beneficial when treating a number of malignancies. They can cause damage to different types of normal cell and organs. Different types of cells are protected by avenanthramide-C (AVN-C). I sought to determine the impact of MTX and CP on hearing and provide details about the possible mechanism of MTX-induced hearing loss because the effects of MTX treatment on hearing loss have not been thoroughly examined. I also wanted to show that the antioxidant AVN-C could protect against ototoxicity caused by these two chemotherapeutic drugs (MTX and CP).

Materials and Methods. Healthy adult C57Bl/6 mice were utilized for this experiments. MTX levels in serum and perilymph were determined by liquid chromatography-mass spectrometry. The groups used in this study were control, MTX, MTX+FA (Folinic Acid), MTX+AVN-C, and MTX+FA+AVN-C, and were evaluated for their effects on the auditory brainstem response (ABR), cochlear synapses, amplitude of wave I, and neuronal integrity. In the MTX-treated group, electron microscopy scanning to examine the outer hair cells (OHCs) was used. In addition, ABR and histology were done to investigate AVN- C efficacy against CP-induced ototoxicity, 3-(4,5-dimethylthiazol-2-yl)-2,5-diphenyltetrazolium bromide and 2,7-dichlorodihydrofluorescein diacetate tests carried off on House Ear Institute-Organ of Corti1

cells (HEI-OC1), and the expression levels of iNOS, IL6, TNF-α, IL1β, BAX, COX2, and HRK were assessed.

Results. After 30 minutes of MTX injection to mice, both the serum and perilymph MTX concentrations significantly rose in mouse body fluids. Hearing thresholds were raised by MTX and decreased by AVN-C and/or FA. The wave I amplitude was reduced by MTX, while it was maintained by AVN-C and/or FA. Substantially, MTX deteriorated the synapses of the cochlea and caused loss of the integrity of the neurons, however AVN-C and/or FA brought protection. MTX diminished cell survival; the level of reactive oxygen species (ROS) in HEI-OC1 cells was increased by MTX, but AVN-C and/or FA lowered these ones. AVN-C preserved hearing thresholds, maintained cell viability, and rescued OHCs from CP-induced damage in the CP-induced ototoxicity model. All tested primers (TNF, IL1, IL6, BAX, HRK, iNOS, and COX2) were highly increased in MTX and cisplatin groups, but suppressed by AVN-C and/or FA. We demonstrated high-dose MTX leading to significant hearing loss. It is thus capable of crossing the blood-labyrinth barrier and destroying cochlear neurons and OHCs. We further demonstrated that AVN-C can prevent hearing loss caused by two chemotherapy medications (MTX and CP) in a mouse model and HEI-OC1 cells.

Conclusion. AVN-C owns protective effects over ototoxicity induced by both MTX and CP, protects the structures of the inner ear (OHCs, neurons, ribbon synapses) against the harm caused by MTX or CP. The action mode of AVN-C towards MTX and CP indicates that ROS are involved in MTX and CP-induced ototoxicity.

1. BACKGROUND OF KNOWLEDGE

1.1. General Cochlear Anatomy

The mammals' hearing organ found in the temporal bone is called the cochlea. It has two important membranes (Reissner's membrane and basilar membrane) that split it up into three parts. Each segment of the cochlea transmits sound waves to the brain uniquely and distinctly. The scala vestibule, and scala media are filled with endolymph and are linked at the cochlea's tip by helicotrema. The required organ in listening (OC=organ of Corti), which is, is located between scala media's outer compartments. This cavity contains the endolymph, which is rich in potassium-ion and poor in sodium-ion accumulation, whereas the outer cavities are occupied with perilymph, which has eventually a high level of sodium and a low level of potassium ion [1]. The image below shows several portions of the cochlea that was photographed using a light source microscope while prepping the cochlea for immunohistology studies (Figure 1).
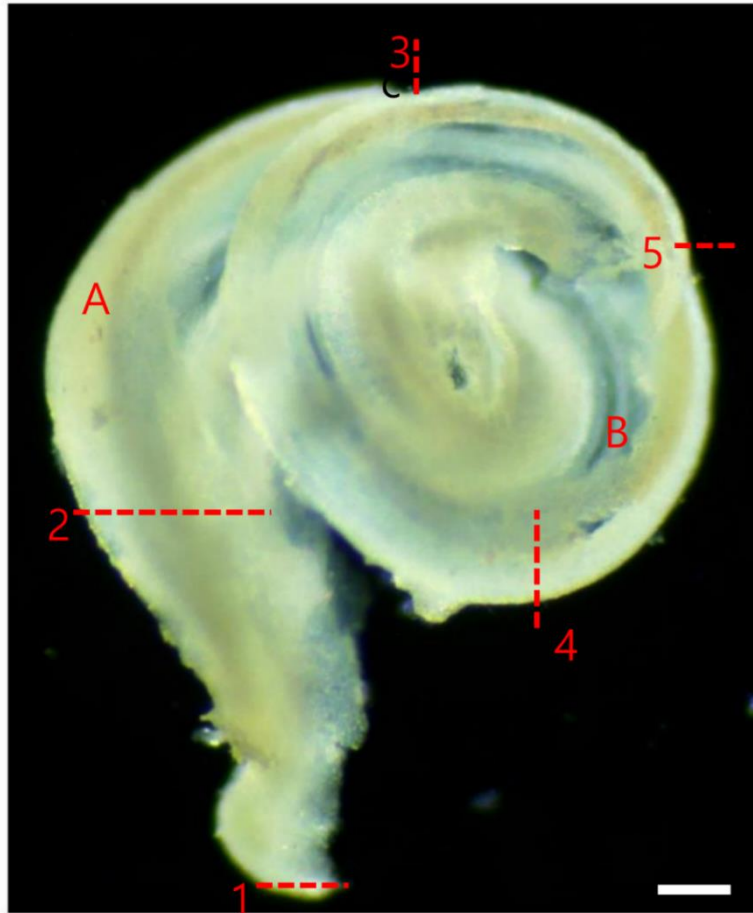
Figure 1. Coiled cochlea image of an adult mouse by light microscope. A light microscope was used to capture an image of an adult mouse's coiled cochlea at 8 weeks of age (magnification x40). The spiral structure of the cochlea is similar to the exoskeleton of a snail. To replicate the architecture of the cochlea, wrap a plastic tube 2.5 times all-around top of a sharpened pencil. This figure depicts the components of the cochlea: from 1 to 2 is the hook region, 2 to 3 is the base turn, 3 to 4 in the middle turn, and 4 to 5 is the apex turn. The points denoted by A and B represent the lateral wall of the cochlea and the OHCs, respectively (in 3 raws). Scale bar indicates 100 µm.

1.2. Discovery and Components of the Organ Corti

The OC is a hearing sense organ identified by Marquis Alfonso Corti an Italian anatomist in 1851 [2]. The organ of Corti (OC), or hearing sensory organ, is dispersed along the partition separating the fluid chambers in the cochlea's coiled tapering tube. Outer hair cells (OHCs), inner hair cells (IHCs), Claudius cells, supporting cells, Deiters' cells, reticula lamina, Hansen's cell, and tectorial membrane make up this organ (Figure 2), which is regarded an essential organ for hearing [3].
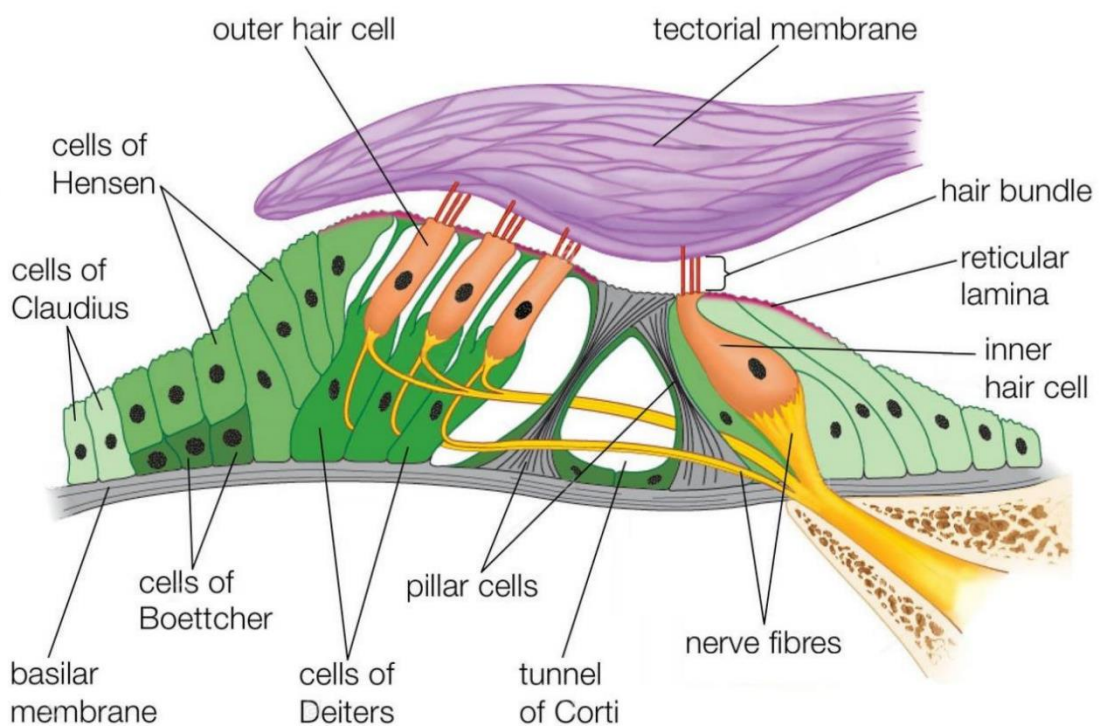
Figure 2. Schematic diagram illustrating different component of of Organ of Corti. Photo courtesy of Images Collection Latin America LLC and Alamy

1.3. The Role of the organ of Corti in ion influx

The movement of the stapes generates vibrations in the cochlea at the basilar membrane. The OC, which is situated on this basilar membrane, detects this vibration movement. Stereocilia of both outer and inner hair cells at their top deflect due to tectorial membrane, which is attached to the limbus, moves. When stereocilia bend towards the kinocilium, the channel at the tip link opens, allowing potassium to enter. Hair cells depolarize as potassium levels rise, and the neurotransmitter is sent via synaptic connections with auditory nerve fibers [4].

1.4. Ribbon synapse components in the inner hair cell

Synapses are built up of multi-units of ribeye proteins with A and B domains in the inner hair cell. The A-domain, which is located inside the synapse, and the B-domain, which extends from the body to the cytoplasm's perimeter, comprise the backbone of the ribbon synapse, resulting in a spherical synaptic ribbon [5, 6]. These two domains are encoded by C-terminal binding protein 2 (CtBP2), which are found in cell nuclei and ribbon synapses in inner hair cells [7, 8].

1.5. The ascending pathway's ribbon synapse has a specific function.

As sounds are continuous, a fast and timely response is essential in the hearing system, and the synaptic ribbon has been identified as a key component of high temporal signal processing [6]. The first control of sound in the auditory ascending route is the synapse located allying inner hair cells and afferent auditory fibers. The inner hair cell's synaptic ribbon can enhance signal transmission in several ways: (1) it gathers a high number of Ca channels, (2) it tethers vesicles to the ready-to-release zone, and (3) it facilitates vesicle replenishment by boosting fusion and priming [9].

1.6. Ribbon synapse types and their characteristics

Ribbon synapses couple with post synaptic dendrites at the bottom of inner hair cells, resulting in ten to twenty ribbon synapses. The spontaneous rate (High and medium) and threshold (High and medium) of these synapses can be distinguished [10]. In a noisy environment, synapses with a high threshold and low spontaneous rate play a crucial role in hearing by masking continuous background noise [11].

2. INTRODUCTION

2.1. Hearing loss, target and risk factors

Numerous damages to auditory organs can cause hearing loss. External auditory stimulation is primarily directed at the OC, a peripheral structure related to signaling transition. Hearing is dependent on the IHCs and OHCs of the OC [12]. Sound is transmitted through IHCs in one level of and OHCs in three levels. After neurotransmitters bind to post-synaptic receptors, the signals transmitted by nerve fibers travel to the spiral ganglion neurons that connect the hair cells to the cochlear nucleus of the brainstem. These accessory inner ear organs are all susceptible to external attack [13]. Noise [14, 15] and ototoxic medications primarily attack hair cells and stereocilia. Damage to these organs prevents signals from reaching the brain from the external ear, resulting in hearing loss. Auditory and spiral ganglion neurons might be primary or secondary targets for external damage [14, 16]. Injury to the myelin or outlying cells of nerve fibers impairs communication, which can lead to encoding issues or inadequate temporal processing [17, 18].

2.2. Hearing loss types

2.2.1. Noise-induced hearing loss

The most preventable cause of hearing loss is traumatic loud sound exposure. According to a recent epidemiological study, noise exposure could put over 600 million people in the world at risk of hearing loss. According to another World Health Organization (WHO) study, noise overexposure is responsible for one-third of all occurrences of hearing loss [19]. Depending on

8

the characteristics of noise, such as strength, frequency, and duration, noise overexposure can cause various sorts of damage to the inner ear. High-intensity traumatic noise can cause permanent threshold shift (PTS), which can be followed by hair cell loss in the Corti organ. Transient threshold shift (TTS) is another type of noise-induced hearing loss. Hearing threshold can recover spontaneously within a few days in this instance; however, a recent animal study found that TTS can accelerate age-related hearing loss in people with normal hearing thresholds [20].

2.2.2. Drug-Induced Hearing Loss

Numerous hearing loss generating medicines have detrimental effect to the inner ear or auditory nerve, leading in hearing impairment. Sometimes the effect of a medicine is only realized after so many months and even years have elapsed. The dose and duration of drug exposure determine ototoxicity. If medication is prolonged, and sometimes even after the medicine is stopped, hearing loss might increase. Poor drug elimination, age, dehydration especially in case of kidney injury, and concomitant administration with more ototoxic medicines are all variables that enhance the risk of drug-related hearing loss. Antibiotics (such as aminoglycosides particularly); anti-cancer drugs (mainly cisplatin); some loop diuretics like furosemide; phosphodiesterase 5 inhibitors like tadalafil are well known to induce hearing loss.

2.3. Oxidative Stress and Auditory Damage

In living organisms, oxidative stress is a normal physiological process where the accumulation of free oxygen radicals surpasses the mechanisms that scavenge them, leading to an imbalance of oxidants and antioxidants. Free radicals were originally found to exist in living cells in 1954, and they have since been linked to the genesis of numerous illnesses. Redox homeostasis, signal transduction, and oxygen concentration all physiologically control the function [21, 22]. ROS and reactive nitrogen species (RNS) (Table.1) According to a considerable body of data in the literature, ROS and RNS are created in a well-regulated manner to assist maintain homeostasis at the cellular level in typical healthy tissues, play a significant role as second messengers, and govern cellular activity by altering signalling pathways. Finally, cells need oxygen to create free radicals and utilise the ATP produced within the mitochondria to do so [23]. Free radicals now become part of the propagative cascade of events, where they combine with other radicals to build additional harmful species, except if the chain is interrupted by antioxidants that stop the cycle to create a benign species [24].

But the term "ROS" has still been frequently used in the literature as a general term for oxidative stress. Although organisms are well-equipped with intrinsic (glutathione peroxidase, superoxide dismutase, catalase, glutathione reductase), and external (uric acid, carotene, C and E vitamins) defences to combat the harm and other effects caused by ROS, to date these defence systems are insufficient in critical situations (UV exposure, oxidative stress, contamination, etc.) where the production of ROS greatly increases.

Table 1. Types of Reactive Oxygen Species

Reactive Oxygen Species (ROS)

Radicals

$O_2^{\cdot-}$	Superoxide
OH.	Hydroxyl
$RO_2^{\cdot}$	Peroxyl
$RO^{\cdot}$	Alkoxy
$HO_2^{\cdot}$	Hydroperoxyl

Non-Radicals

H_2O_2	Hydrogen peroxide
HOCl-	Hypochlorous acid
O_3	Ozone
$^1O_2$	Singlet oxygen
$ONOO^-$	Peroxynitrite

2.6. Methotrexate

Methotrexate (MTX), formerly known as amethopterin, is currently an anticancer drug that also has immunosuppressive properties. MTX has antimetabolite and antifolate effects, as well as immunomodulatory activities against several inflammatory illnesses. It works by inhibiting the enzyme dihydrofolic acid reductase, which affects the metabolism of folate, by stifling the synthesis of purines and pyrimidines, and by delaying the synthesis of DNA and RNA. Many works have examined, understood, and reported on its pharmacokinetics and potentially harmful consequences such as hepatotoxicity and nephrotoxicity [25, 26]. For decades, MTX has been used efficiently and extensively to treat numerous tumors in medicine. Studies have shown that MTX enhanced the production of ROS in monocytes and cytotoxic T cells, which decreased the ability of monocytes to adhere to endothelial cells. High-dose MTX (HD-MTX) generated temporary neurotoxicity in the form of white matter injury in patients with acute lymphocytic leukemia [27, 28].

Previous study showed that 60 percent of children aged 5 and under who got MTX treatment and had their brainstem auditory system examined in earlier trials with acute lymphoid leukemia showed auditory loss [29, 30]. In order to confirm ototoxicity in chemotherapy patients, a brainstem auditory-evoked potential screening was performed. The results showed that a significant portion of those evaluated had some kind of change and latency delay, with auditory impairment in the lower brainstem being the most common. Additionally, MTX and other cancer drugs administered simultaneously while treating both solid and hematological malignant tumors led to ototoxicity [31, 32].

2.7. Cisplatin and Ototoxicity

Chemotherapy based on platinum-containing anticancer medications such as cisplatin and carboplatin [33]. Some more chemotherapy drugs include nitrogen mustard, amino-nicotinamide, dichloromethotrexate, bleomycin, and 5-fluorouracil. For instance, cisplatin contains four ligands that are cis-positioned pairs of chlorine atoms or amine groups in addition to a divalent Pt (II) core atom [34]. A wide variety of malignancies are successfully treated with cisplatin, however due to its ototoxic potential, cancer patients who are exposed to it run the risk of hearing loss, which can further impair the patients ' quality of life [35]. Cisplatin has been well studied compared to MTX and its ototoxicity has been well documented. During high-dose (100-120 mg/m^2) cisplatin treatment, 54 patients with metastatic cancer were monitored audiometrically. After therapy, 81 percent of the patients had significant changes in air-conduction hearing thresholds. Thirteen percent had a substantial hearing impairment [36]. Additionally, in a study of 277 individuals on statins who were treated with cisplatin for head and neck cancer, hearing loss caused by cisplatin was found to be more common with greater thresholds among patients on concurrent atorvastatin compared to nonstatin users [37].

2.8. Definition of Antioxidants

Antioxidants are substances, either manufactured or natural, which can effectively prevent or postepone cell damage [38]. Due to the health benefits of diets rich in fruits and vegetables, which are powerful sources of antioxidants, antioxidant supplements are helpful in the prevention of disease. Examples of antioxidants include the selenium, vitamins C and E, carotenoids including lycopene, zeaxanthin, lutein, and beta-carotene as well as oats [39].

2.9. Discovery of Antioxidant agents

Many researchers have reported beneficial effects from herbal items, and epidemiological studies have revealed a link between the whole grain diet and chronic diseases. Phytochemicals with antioxidant capabilities found in cereals have been demonstrated to protect cells from oxidative damage in published studies [40]. According to various publications, antioxidants are essential in the prevention of human disease. Antioxidant-active compounds can work as reducing agents, singlet-oxygen quenchers, pro-oxidant metal complexes, and free radical scavengers. As a result, antioxidants are gaining popularity, as they may help to prevent age-related deterioration, heart disease, membrane damage, and cancers [38].

2.10. The History and Health Benefits of Oats (Avena sativa L.)

According to studies, oats (Avena sativa L.) have indeed been farmed for over thousands of years and were used not only as a feeding plants for animals but also in a wide range of foods for human consumption [41, 42]. Consumption of oat-based products has numerous health benefits [43, 44]. Oats have been shown to help bring down plasma cholesterol, enhance glucose and insulin control, and minimize the risk of coronary heart disease due to their high nutrient content, which contains high levels of dietary fibers like ß-glucan, minerals like calcium and iron, lipids, vitamins like vitamin E, proteins, and a wide variety of antioxidants [45, 46]. There has also been a lot of attention on how phenolic amides from plant-based foods affect human health [47, 48]. Antioxidant qualities and possible therapeutic benefits of phenolic amides include anti-inflammatory, antiproliferative, and antigenotoxic effects [49, 50].

2.11. Avenanthramides and Their Subclassifications

Avenanthramides (AVNs) seem to be lower molecular weight polyphenols present exclusively in oats which serve as phytoalexins generated in response to infections [51]. These compounds belong to the hydroxycinnamoylanthranilate alkaloids, which are only found in oats. Over 25 AVNs compounds have been found, but the three most common are AVN-A, -B, and -C, which differ only by hydrogen, hydroxyl, or methox on the C-3 of the cinnamic acid residue in each fraction [52] (Fig3).
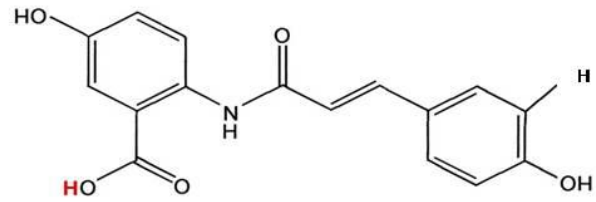
Avenanthramide-A
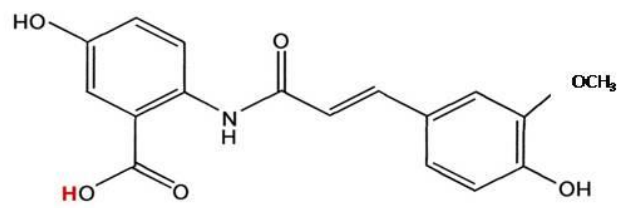
Avenanthramide-B
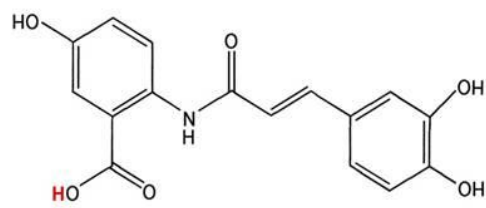
Avenanthramide-C

Figure 3. Chemical structures of major types of Avenanthramides

In vitro, all three AVNs displayed antioxidant activity, with the order of activity being proportional to the amount of hydroxycinnamic acid residue in each fraction [53]. Antioxidant properties in AVNs has already been reported *in vitro* and *in vivo*, with Avenanthramide 2c (AVN-C) has the strongest antioxidant capacity, making it a potential therapeutic choice for a variety of conditions [14, 30].

In the last ten years, research on the impact of dietary polyphenols on human health has progressed significantly. It strongly indicates that polyphenols safeguard against degenerative diseases such as cancer and cardiovascular problems. The antioxidant effects of polyphenols have been extensively explored, however it has become obvious that polyphenols' methods of action extend beyond oxidative stress control [40, 54].

2.12. Purpose of the Research

This study set out to see if AVN-C could guard against ototoxicity brought on by anti-cancer medications (methotrexate or cisplatin), as well as to learn more about the mechanisms involved and to look into the toxic effects of MTX on normal hearing using both in vivo and in vitro studies, by treating these various drugs and then observed and measured the outcomes.

3. MATERIALS AND METHODS

3.1. Animal care and reagents

In this investigation, male and female C57Bl/6 strain mice ranging from 4–6 weeks old were used and three mice per group were considered. The vivarium was maintained according to standard mouse husbandry guidelines, and the proper food and water being given. The Institutional Animal Care and Use Committee at Chonnam National University gave the study their support and approval (CNUHIACUC-20027). Measurement recordings and surgery procedures were conducted after animals were given anesthesia to minimize pain. The molecules utilized in this research were Cisplatin (CP, Korea united Pharm.inc, For the Best Pharmaceutical Company, South Korea Republic), Methotrexate (Sigma-Aldrich MTX; St Louis; MO 63178; Cat. M9929; USA), Folinic Acid calcium salt (FA, Cat. 47612, 3050 Spruce Street, St Louis MO63103, Sigma, USA), and Avenanthramide-C (AVN-C, Kind donation from Professor Jong Hyun Cho), were given to the mice as shown in figure 4. (4A) AVN-C, FA and MTX treatment protocol. (4B) AVN-C and CP treatment protocol.
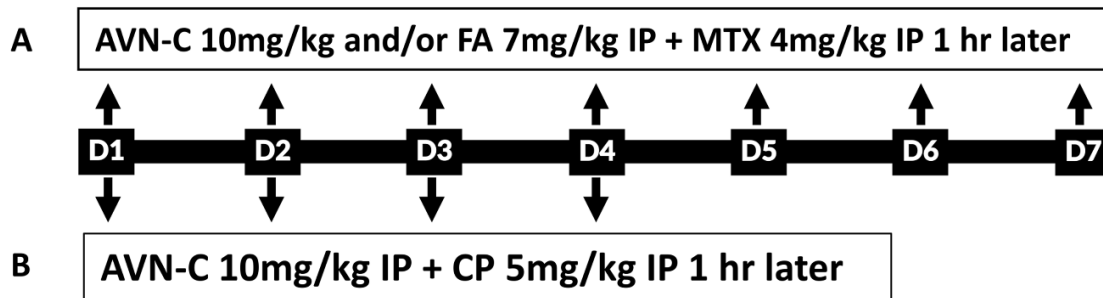
Figure 4. Drug delivery in mice is illustrated schematically. (A) administration of MTX, FA, and/or AVN-C. For seven days, mice received MTX 1 hour after receiving either AVN-C or FA alone or in conjunction. (B) For four days, AVN-C was given one hour before to CP.

3.2. Methotrexate Measurement in Mouse Body Fluids to Assess Drug Levels

The MTX used in this study investigation was soluble in 0.9 percent normal saline both for *in vitro* and *in vivo* applications. To check the concentration of MTX in mouse biological fluids (perilymph and serum), subjects were given intraperitoneally (IP) 4 mg/kg of MTX, whereas controls received normal saline, the carrier. Following anaesthesia, whole blood was removed from mice through cardiocentesis and stored in an Eppendorf tube (EP) left for 30 minutes in an upright position to congeal the blood. The serum was then extracted fast at 20 degrees, 1500g for 10 minutes, and sent for Liquid Chromatography-Mass Spectrophotometry (LC-MS) to determine MTX concentration.

The mice were put to sleep before having their heads connected to a mouse head holder in order to collect perilymph. The subcutaneous fat covering was removed after the surgical incision, and the muscles were then carefully dissected to reveal the tympanic bulla. With a gentle

19

removal of the fragments of the bone, before the round window niche was revealed, the bulla was unwrapped. To harvest perilymph, a glass pipette was carefully put into the hole in the round window. Liquid chromatography-mass spectrometry (LC-MS/MS, Shimadzu LC 20A System, AB SCIEX 4000 Q Trap mass spectrometer, USA) was used to detect MTX in all fluids. Ion Spray Turbo at 500°C, 5500 V, positive mode, MRM scan form, GS1 50, CG 20, GS 60 spray voltage (Loperamide m/z 477.223/266.200, MTX m/z 316.169/163.000), MS status was employed. Local conditions were presented as follows: 40°C column oven, 150 mm X 3.0 mm fitted with Gemini C18 guard cartridge (4.0 mm X 2.0 mm), Gemini C18 3.0 m, and 4°C autosamplers. Phase mobile ACN- DIW 40:60 (V/V) together with 0.1 % carboxylic acid and a rated flow of 0.3 ml/min. The usual MTX stock solution used in the 0.9 percent Normal Saline and Loperamide solution was 1 mg/ml.

3.3. Assessing animal hearing by auditory brainstem response

We assessed the ABR from click and tone burst stimuli one month following drug treatments. The ABR in the left and right ears was assessed, and the body temperature was kept using a heat therapy pump (Cat.TP700, Michigan, 380 Centre East Avenue 49002, USA). Mice were made to sleep for the smooth recording by an intraperitoneal injection of ketamine (120 mg/kg) mixed with xylazine (10 mg/kg), and each mouse was placed in an audiometric chamber for ABR recording. As previously reported, these ABR tone burst frequencies were checked: 8-16-24-32 kHz [30, 55]. The free field used to evaluate the hearing range of mice, rats, and guinea pigs were optimized using TDT's MF1 Multi-Field Magnetic Speaker [30, 56]. The stimulus intensity levels were examined at each frequency in decreasing order, i.e., from 90 dB to 20 dB of the visual ABR threshold. A custom-made probe tube microphone was used to calibrate the stimulus level at the ear opening.

3.4. Wave I Analysis

To find the lowest intensity at which an ABR wave I was recognized, the acquired ABR thresholds were reduced in stimulus intensity by 20 dB for each studied group. Analysis of the stacked waveforms with the help of the program R (Free Software Foundation's GNU General Public, version 4.0.4, Austria) yielded the ABR thresholds and amplitude of wave I. The large amount of ABR data collected was kept on external drives for later offline analysis of the amplitude and latency of the ABR components. The amplitude of Wave I at 90 dB SPL was taken to be the magnitude difference between the first positive peak and the following negative peak.

3.5. Scanning electron microscopy

To minimize the length from death and fixation at room temperature (RT) (typically 2 minutes), the cochlea was promptly removed from the mouse bone cement (one mouse each) and a puncture was made at the apical turn of the cochlea. Two-point five percent glutaraldehyde in 0.1 M sodium cacodylate buffer comprising 4 percent paraformaldehyde (PFA) (500 µL) was carefully perfused via the open round window, exiting through the formed hole at the apex turn. After that, the tissues were postfixed up for a night at 4°C on a circular path with the same buffer, rinsed with distilled water, and decalcified for two hours in 5 percent ethylenediaminetetraacetic acid (EDTA) in 100 mM Tris, pH 7.4 at 4℃ gentle rotations. The

cochlear turns were sliced and detached from the surrounding membranes before being post-fixed for 2 hours at room temperature in 1% osmium tetroxide at 4°C. The samples were then sequentially ethanol rinsed from 50% to 100% ethanol, then evaporated at the crucial moment,

placed on carbon header supporting inserts, and sputter encased using silver. A scanning electron microscope (EM-30AX Plus COXEM, South Korea Republic) with a beam energy of 15 kV was used for imaging.

At a magnification of 500X, the number of outer hair cells in the cochlea was counted for each turn of the cochlea. The number of outer hair cells in 100 μm cochlea turn length was averaged for each group. A hair cell was regarded as nonexistent if the bundle of stereocilia was lacking.

3.6. Cochlear neuron integrity and outer hair cells

A gaping tear was created exactly at the cochlea's proximal turn. Following that, 4 percent PFA was delivered through the circular window to the apex turn of the cochlea, followed by 4 hours of post-fixation with moderate rotation at 4°C. In contrast to bone decalcification, the cochleae were immersed in 0.12 mM EDTA at 4°C for 1 hour. Three tiny pieces were cut from each cochlea (apex, middle, base). The tissue specimens were soaked in blocking buffer (donkey serum: 0.1 percent PBS-T, 1:100 dilution) for 1 hour at room temperature before being treated with primary antibodies up overnight at 4°C. Secondary antibodies were added at RT for 3 hours after washing three times with 0.1 percent PBS-T (with 30 minutes between each washing). The samples were then stained with phalloidin and 4′,6-diamidino-2-phenylindole (DAPI) for 3 minutes and rinsed once in PBS for 30 minutes according to the study protocol. Afterward, the specimens were put on a glass plate with vector protection solution and covered with a glass cover, then examined with a laser scanning microscope LSM 800 (Jena Promenade 10.07745, Carl Zeiss, GmbH Microscopy, Germany). These secondary antibodies were utilized: Anti-Neurofilament 200 (NF200, Abcam, #8135, 1:100), Phalloidin (PL, Cell

signaling, # A12379 1:5,00), and DAPI (Invitrogen, 1:1000), Presitin (MyBioSource 1:100, #MBS423494), and Calbindin (Invitrogen, WC3214704E, 1:100).

3.7. Estimation of the number of inner hair cell presynaptic ribbons

The number of IHC ribbon synapses from the cochlear apex, middle, and basal turns was determined. Counts were performed from top to bottom in the cochlea. Across each basal turn, we selected three visual fields containing 10–12 IHCs. In each group, we selected three samples to estimate the average number of ribbon synapses in IHCs. The IHC ribbon synapses were identified following staining with C-terminal binding proteins 2 (CtBP2, # 612044, 1:100, BD Transduction Laboratories™), myosin-7a (1:200, # 25-6791, Proteus), and the image was taken with a Carl Zeiss microscope as previously described.

We selected three areas of 20 μm of the chosen turns of the cochlea and delineated these with a square in all studied groups. We examined presynaptic ribbons (CtBP2 signals) of the IHCs that were identified surrounding IHCs and within nuclei and estimated the number of presynaptic ribbons per IHC.

3.8. In vitro investigation with HEI-OC1 cell

HEI-OC1 cells were grown in a permissive environment (33°C). Dulbecco's Modified Eagle Medium-high glucose was used as the media (Gibco, Gaithersburg, USA). The media contained 10% nonantibiotic fetal bovine serum (Gibco BRL) and 50 U/mL gamma interferon (Cambridge, MA- Genzyme, USA). To elicit cytotoxic effects on HEI-OC1, AVN-C was

diluted in Dimethyl sulfoxide (DMSO) and administered at a dose of 1 μM; MTX was

dissolved in 0.9 percent normal saline and administered at a dose of 0.2 μM. Distilled water

was used to dissolve FA and given at a dose of 3 μM, CP at a dose of 30 μM. The treatments

of AVN-C and/or FA were done 3 hours before MTX or cisplatin injection.
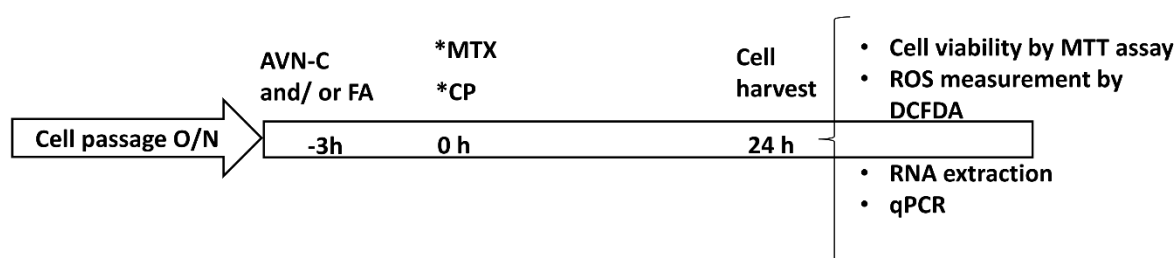
Figure 5. Schematic representation of drug administration to HEI-OC1 cells

Overnight, HEI-OC1 cells were grown. Cell culture was administered AVN-C 1 μM alone or

in combination with FA 3 μM 3 hours before MTX. AVN-C 1 uM was administered to cells

three hours before CP 30 μM and incubated for 24 hours at 5% CO_2, 37°C before being

employed in various studies.

3.9. MTT staining for cell survival assessment

To make a reagent for this test, 25 mg of Thiazolyl Blue Tetrazolium Bromide (#M2128 MTT,

Sigma-Aldrich, USA) was diluted in 5 mL of PBS. Each well received 20 μL of this reagent

and incubated for 30 minutes at 37°C. Finally, for each sample, 100 μL of DMSO was used.

The samples were kept for 4 hours at 37°C incubation and were then examined. The absorption

spectrum of formazan in the mixtures was determined utilizing a spectrophotometer glass cuvette machine (#202-6262, SpectraMax ABS Plus-Molecular Devices, USA). All calculations were made inside the plate reader by running experiments in 96-well plates, and the average transmitted density in control cells was considered for being 100%.

3.10. ROS measurement

An ROS Detection Assay Kit (D399, Invitrogen) that is designed to examine ROS in HEI-OC cells after drug treatment was used for this measurement. At 37°C, 5% CO_2 incubator with humidity the cells were left for 30 minutes then resuspended. The cell-permeable reagent dye, which is a fluorogenic dye to quantify peroxyl, hydroxyl activity, and other ROS in the cell, was used [57]. Stained HEI-OC cells were washed one time in 1X buffer and placed in a microplate reader, and the luminescence was measured using a flow cytometer device (495 nm/ 529 nm, excitation/emission wavelengths – Biosciences, BD FACSCaliburTM, USA). With Kaluza Analysis Software, ROS variation was reported as a proportion of control after background subtraction (Coulter Beckman, Brea Inc, USA).

3.11. Extraction of RNA and RT-PCR

After harvesting treated HEI-OC1 cells, total RNA was obtained using the reagent TRIzol (Invitrogen). The concentration of RNA was conducted using a spectrophotometer device (ND-1000, Wilmington, Technologies Inc., USA) with the measured absorbance at excitation/emission of A260/A280 nm.   The results were analyzed using ND-1000 software. A reverse transcription cDNA synthesis package was used to create homologous first strand

DNA (cDNA) from RNA (1st strand cDNA Synthesis kit, 6110A, Takara PrimeScriptTM, Japan). For RT-PCR, Taq Master Mix was adopted (Bioscience, Germany). The experiments were performed by differently 3 times. Denaturation took place at 95°C for 10 minutes and 10 seconds, followed by annealing at 62°C for 20 seconds and 72°C for 30 seconds in 60 cycles. The list of used primers for each gene is shown in table 2 below as follows:

Table 2. Primer sets for real-time, quantitative polymerase chain reactions

Genes	Primers	Size (Bp)	Annealing temperature (℃)
GAPDH	Forward: 5′-ACCACAGTCCATGCCATCAC-3′	20	60.1
	Reverse: 5′-TCC ACC ACC CTG TTG CTG TA-3′	20	
IL-1β	Forward: 5′-GCTGCTTCCAAACCTTTGAC-3′	20	59.86
	Reverse: 5′-AGGCCACAGGTATTTTGTCG-3′	20	
IL-6	Forward: 5′-TCCAGTTGCCTTCTTGGGAC-3′	20	53.8
	Reverse: 5′-GTACTCCAGAAGACCAGAGG-3′	20	
TNF-α	Forward: 5′-CCACCACGCTCTTCTGTCTA-3′	20	58.1
	Reverse: 5′-CACTTGGTGGTTTGCTACGA-3′	20	
BAX	Forward: 5′-CTACAGGGTTTCATCCAG-3′	18	63
	Reverse: 5′-CCAGTTCATCTCCAATTCG-3′	19	
HRK	Forward: 5′-ATTCCGTACCTGTGCATGCCTG-3′	22	64
	Reverse: 5′-TGTGCTGAACAGTTGGTCCACG-3′	22	
iNOS	Forward:5′GCATGGAACAGTATAAGGCAAACA-3′	24	62
	Reverse: 5′-GTTTCTGGTCGATGTCATGAGCAA-3′	24	
COX2	Forward: 5′-GCATGGAACAGTATAAGGCAAACA-3′	24	62
	Reverse: 5′-GTTTCTGGTCGATGTCATGAGCAA-3′	24	

3.12. Data analysis

One-way analysis of variance was used and conducted using GraphPad Prism version 8.0. Each experiment was performed three times, and a p-value of 0.05 was considered significant. The data are presented as mean ± standard deviation.

4. RESULTS

4.1. Following systemic injection, MTX crosses the blood-labyrinth membrane.

To see if MTX has a direct influence on the cochlea, we looked for it in the cochlear fluid after systemic treatment. To accomplish this, mice were given 4 mg/kg of MTX single dose (IP), and blood was drawn at various time (30 min, 1, 2, 3, 6, and 8 hour) and processed by liquid chromatography-mass spectrometry (LC-MS/MS) to measure the quantity of MTX in the serum (Fig.6A). Figure 6B showed that the blood serum level of MTX in wild-type (WT) mice peaked at $1,490 \pm 2.8$ ng/mL 30 minutes after IP treatment and then rapidly decreased.

To test if MTX crosses the blood-labyrinth barrier (BLB), the concentration of MTX within perilymph was assessed across many time intervals (1, 2, and 3 hours) post IP injection of MTX in wild type mice. MTX concentration in the perilymph reached 93.2 ± 4.2 ng/mL one hour after injection, indicating that MTX passed through the BLB. The amount of MTX inside the perilymph was much lower after 2 and 3 hours (Fig.6C).
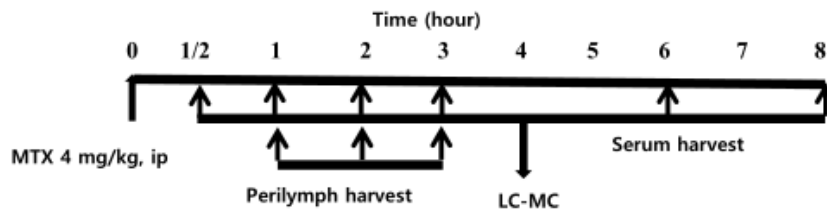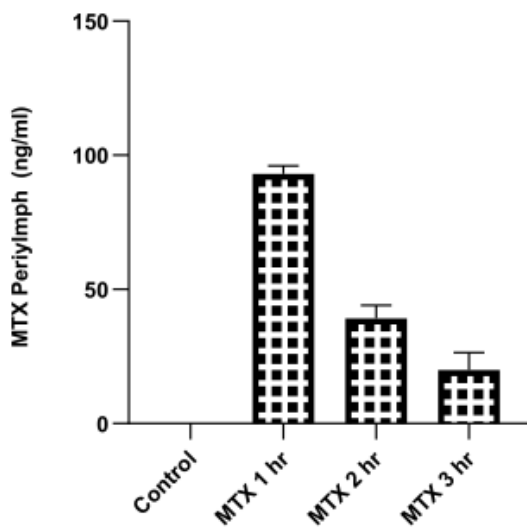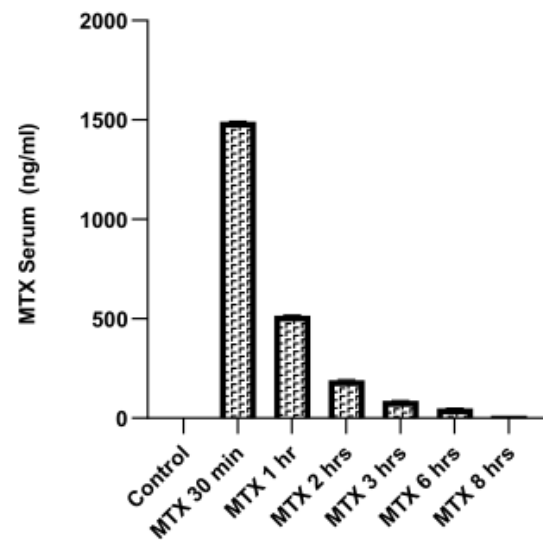
Figure 6. **Measurement of methotrexate in mouse body fluids.** Time and treatment plan of MTX in mice is depicted. 0 hour indicates the beginning of injection 4 mg/kg of MTX to animals through IP injection; ½, 1, 2, 3, 6, and 8 hou**r** reflect serum collection intervals; and 9 hour show LC-MS timeline (uppermost). Regarding perilymph, 1, 2, and 3 hours indicate perilymph sampling points in time (bottom); whereas 4 hours signify the LC-MS timeline to assess the availability of MTX in the perilymph. Serum and perilymph were gathered and analyzed in Panel A. After 30 min, MTX concentrations inside the serum rose and thereafter progressively fell, indicating that MTX is absorbed by diverse tissues. Panel B: MTX was identified within perilymph 1 hour after injection and steadily declined over the next few hours. Panel C. Each group used three mice for this experiment. Published   data. Plos One DOI: 10.1371.

4.2. Audiometry Brainstem Response (ABR)

4.2.1. *In vivo*, high-dose MTX triggers significant hearing loss.

During an *in vivo* experiment, high-dose methotrexate (HD-MTX) led to an increase in hearing thresholds in mice given just MTX. In Control mice, one-month post-treatment, the hearing thresholds for click and tone burst sounds increased (65 ± 11.5 and 79.8 ± 10.3 dB SPL) (Fig.7B, C).

4.2.2. Hearing is protected from MTX ototoxicity by AVN-C and FA

The efficacy of AVN-C and FA against HD-MTX-induced ototoxicity was investigated. Being given 1 hour before MTX administration, AVN-C and FA effectively diminished the hearing thresholds for click sounds in WT mice (21.4 ± 2.4 dB and 28.9 ± 3.9 dB SPL, respectively) (Fig.7B). The hearing thresholds for tone bursts were also decreased by AVN-C and FA (23.5 ± 3.8 dB and 37.3 ± 6.7 dB SPL) (Fig.7C). Concurrent injection of AVN-C and FA 30 min before MTX treatment ended up in hearing thresholds declines of 23.6 ± 2.4 dB SPL for click sounds (Fig.7B) and 26.7 ± 6.2 dB SPL for tone burst (Fig.7C). The hearing threshold for tone bursts of the AVN-C and FA-treated groups declined at each recorded frequency, according to my findings of the ABR (Fig.7C).
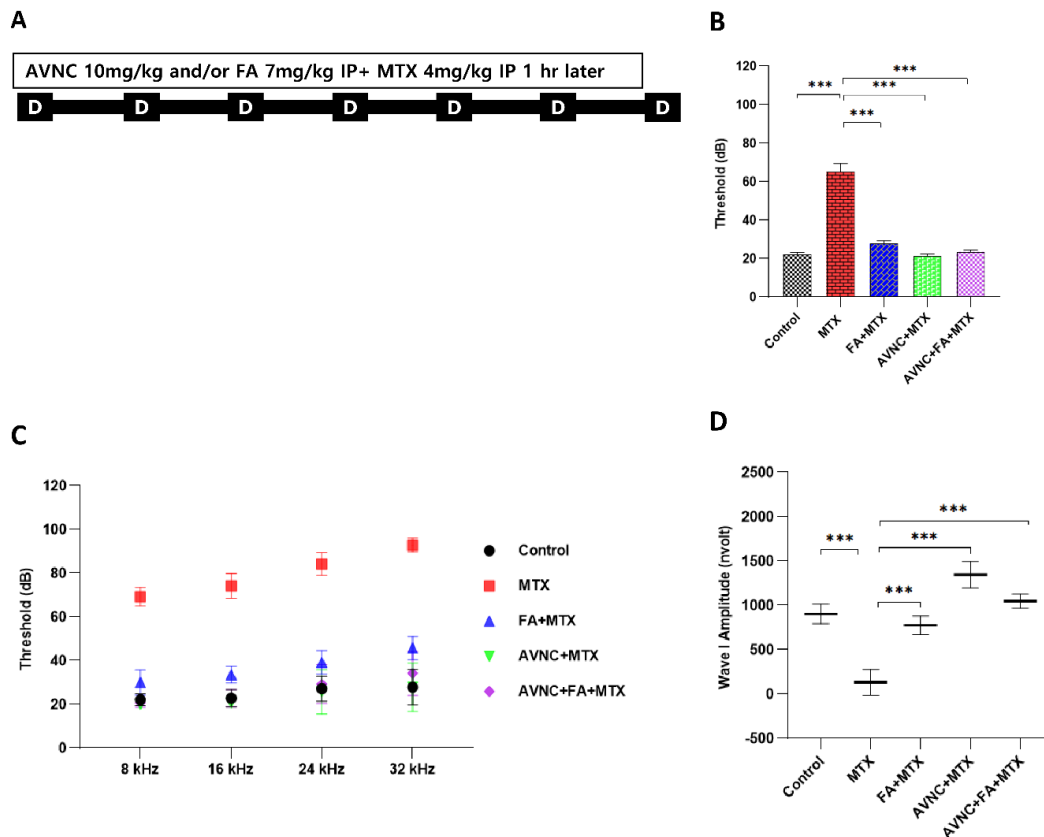
Figure 7. AVN-C and FA protect hearing from MTX-induced ototoxicity. A timeline and conceptual design of drug treatment are shown in the diagram below. For 7 days, AVN-C and FA were injected IP 1 hour before MTX administration. Panel A. The click sound showed that MTX increased hearing thresholds one month later, whereas AVN-C and FA treatment preserved the threshold shift. Panel B. The threshold results (both click and tone bursts) of the AVN-C group were identical to those of the control group. Panel B and C: ***$p < 0.001$ (one-way ANOVA). The dominant wave component is marked I at 90 dB SPL. The wave I amplitude was calculated using the stacked waveforms. The magnitude difference between the first positive peak and the second negative peak was designated as the amplitude of Wave I. The MTX caused a decrease in the wave I amplitude. AVN-C and FA maintained the wave I amplitude high (p-value < 0.001; one-way ANOVA), and AVN-C alone surpassed both FA alone and AVN-C/FA combined. Panel D. Published   data. Plos One DOI: 10.1371.

4.2.3. AVN-C improves hearing in Cisplatin-induced ototoxicity

The preventive and alleviative effects of AVN-C on cisplatin-induced ototoxicity were investigated using a mouse model. In the control and AVN-C groups, results indicated that AVN-C treatment in normal mice has no effect on hearing ability; however, the cisplatin group showed significant changes in ABR threshold, confirming that cisplatin treatment causes significant hearing loss (Fig.8B, C).

The administration of AVN-C to mice one hour before Cisplatin was shown to protect the mice's hearing. Changes in ABR threshold were less than 20 dB in the click sound (Fig.8A) and in the entire frequency range below 40 dB SPL (Fig.8B).
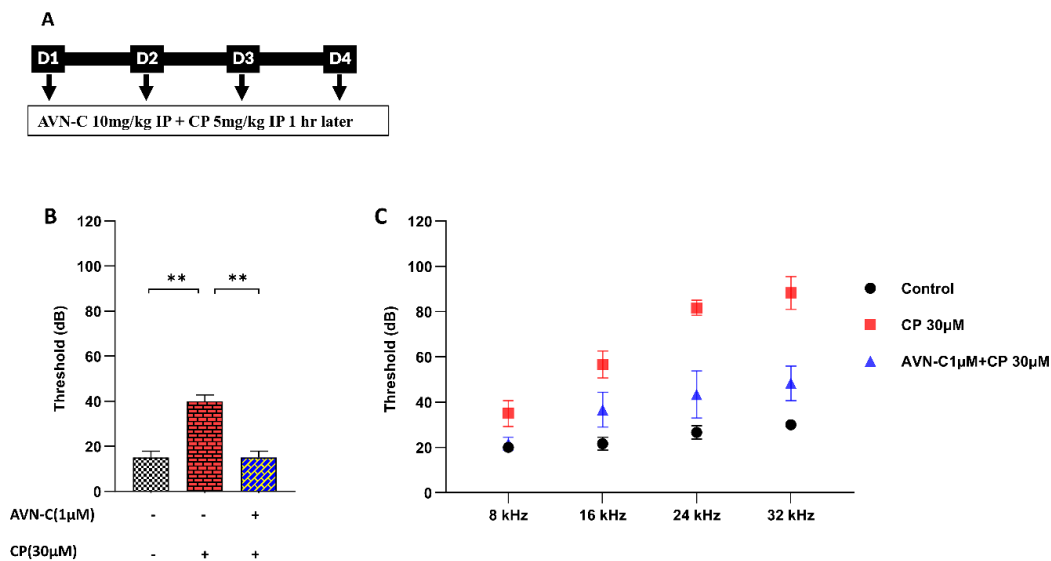
Figure 8. Hearing ability assessment in cisplatin-injected mice receiving AVN-C. To assess hearing abilities, researcher examined changes in ABR threshold using transient click and tone-burst (8, 16, and 32 kHz) stimuli in three animal groups. The results are presented as means standard error of the mean. P-value was significant *p< 0.05 when compared to the control group.

4.3. Methotrexate damages OHCs while AVN-C and FA protect OHCs

We looked for damage to the outer hair cell (OHC) stereocilia to see if AVN-C protected auditory hair cells from MTX-induced ototoxicity. A normal cochlea was compared to a treated cochlea 1 month following systemic administration of MTX, AVN-C, and FA using scanning electron microscopy (SEM). Several OHCs were destroyed in the MTX-treated group compared to the other groups (Fig.9A), and OHC damage was found mostly at the base (14 ± 6 OHCs), middle (19 ± 5 OHCs), and apex (20 ± 4 OHCs) turns of the cochlea (Fig.9B, C, D). Some missing OHCs were identified in the FA+MTX-treated group at the base (38 ± 2), middle (39 ± 5), and apex (40 ± 7) turns (Fig.9A, B, C, D). Moreover, AVN-C shielded the OHCs at the base (49 ± 2), middle (49 ± 2), and apex (51 ± 3) turns (Fig.9A, B, C, D). The co-administration of AVN-C and FA reduced the lethality of MTX on OHCs to 42 ± 4 OHCs at the base turn, 43 ± 5 OHCs at the middle turn, and 43 ± 4 at the apex turn (Fig.9A, B, C, D). Ototoxic medications, as well as noise, have been shown to affect these OHCs. The number of OHCs in the control group that received the carrier was as follows: base turn, 44 ± 2 OHCs; middle turn: 43 ± 4 OHCs; and apex turn: 43 ± 5 OHCs (Fig.9A, B, C, D). The OHCs number per 100 μm was calculated, and a p-value of 0.001 was judged significant across all experimental groups. Furthermore, the inner hair cells (IHCs) looked to be normal and well kept.
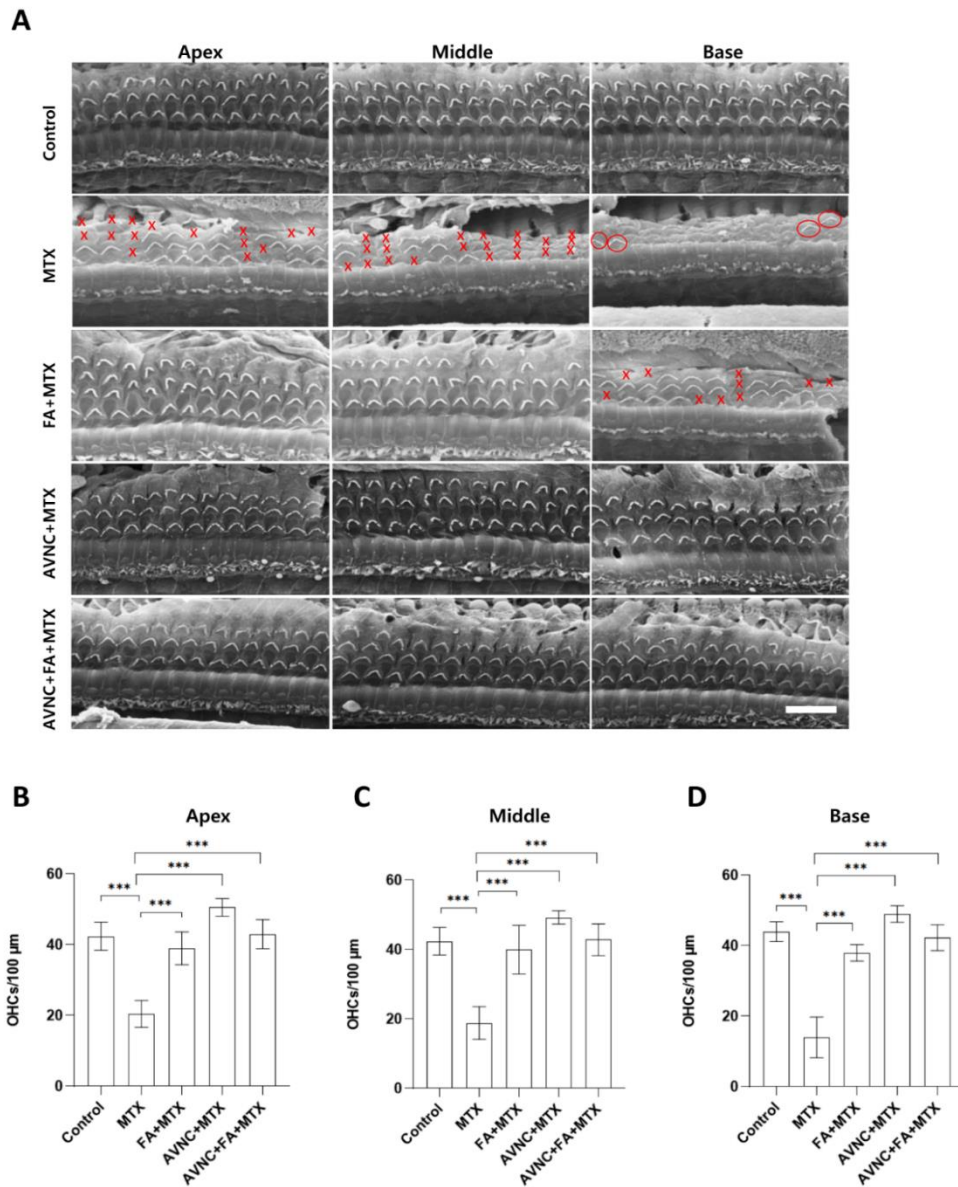
Figure 9. MTX administration induces OHC destruction, whereas AVN-C and FA retain OHCs in the mouse cochlea. MTX significantly destroyed the OHCs in all cochlear turns. Panel A: When given before MTX, AVN-C and FA safeguarded the OHCs. Panels A, B, C, and D show that AVN-C injection contributed to the retention of more OHCs at the cochlea turns than FA. Panels A, B, C, and D: p-value < 0.001; one-way ANOVA. In the illustration, O represents the presence of OHC (red color) and X symbolizes the absence of OHC. Scale bar indicates 100 µm. Published   data. Plos One DOI: 10.1371.

4.4. AVN-C ensures hearing capacity and represses tangible cell death from cisplatin-induced ototoxicity

To determine whether the hair cells were affected by cisplatin-induced ototoxicity, whole-mount Prestin (Pres) and calbindin (CBD) staining of the organ of Corti was performed. As a result, we found that cisplatin caused significant degeneration of outer hair cells at all three cochlea turns base, middle, and the apex (11.7 ± 2.9, 17.3 ± 4.2, 20.0 ± 5 OHCs) (Fig.10A, B, C). Especially the area of the basal turn showed more severe damage than the areas of the middle and apical turns, and outer hair cells were more susceptible to cisplatin as inner hair cells looked normal. The pre-treatment of AVN-C one hour before CP protected OHCs from the damage caused by cisplatin (36 ± 2, 43.3 ± 2.1, 42.3 ± 3.2 OHCs) (Fig.10A, B, C). The staining of Prestin alone (red) shows in full detail the magnitude of OHCs loss and the way AVN-C safeguarded OHC (Fig.10B). The number of IHCs remained intact (Fig.10D).
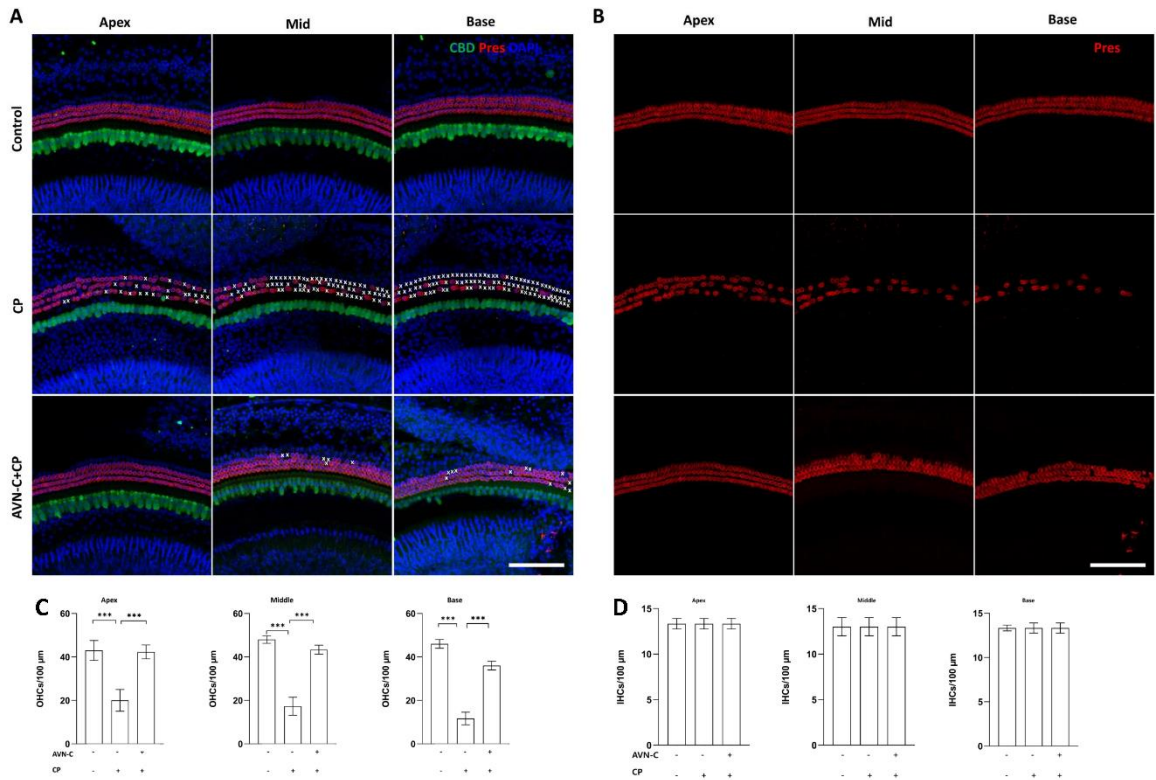
Figure 10. The effects of AVN-C on cisplatin-induced hair cell damage in mouse cochlea mice.
The OC was stained whole mount to establish the protective effects of AVN-C against cisplatin-induced ototoxicity in hair cells. (A) The organ of Corti, comprising inner and outer hair cells, was stained with Prestin (red), CBD (Calbindin green), and DAPI (blue) to confirm hair cell viability or degeneration. Degenerating outer hair cells are shown by white asterisks. (B) OHCs are shown stained with only Prestin to indicate the severity of the loss of OHCs. (C) and (D) The quantification of the number of inner and outer cells in each animal group at the basal, middle, and apical turns of the cochlea using a histogram is presented. The data are shown as means SD. *p<0.05 when compared to the CP group and three mice were used per group. CP (Cisplatin), CBD (Calbindin), OHCs (outer hair cells), IHCs (inner hair cells). Scale bar indicates100 µm.

4.5. AVN-C administration spares ribbon synapses from MTX-induced damage.

Synapses from cochlear whole-mount extracts from mice sacrificed shortly following ABR recordings were labelled with RIBEYE/CtBP2 and quantified to properly dependent variable assumptions: (1) AVN-C reduces synapse reduction, and (2) MTX induces synapse damage in the cochlear IHC areas. The synapses in cochlear areas corresponding to the investigated stimulus frequencies that activated ABR were recorded. MTX destroyed and lowered the number of IHC-band synapses across the cochlea, according to the findings (Fig.11A). The MTX-treated group's CtBP2-positive signal count showed a lower number of synapses in all three turns of the cochlea: apex (21.7 ± 8.3), middle (18.7 ± 5.9), base (13.4 ± 2.6) (Fig.11B, C, D). The AVN-C-treated group, on the other hand, maintained many cochlear synapses. at the apex (53.7 ± 4.9), middle (53.4 ± 2.4), base (52.3 ± 3.9) turns (Fig.11B, C, D). The proportion of cochlear synapses was higher in the FA+MTX-treated population (48.8 ± 5.3, 44.7 ± 6.8, 44.1 ± 6.9, respectively), AVN-C+FA+MTX-treated group (51.1 ± 6.3, 49.7 ± 6.9, 51.8 ± 6.8, respectively), and control group (49.1 ± 5.6, 43.3 ± 5.8, 44 ± 4, respectively) in the apex, middle and base turns and significantly (***$p < 0.001$) (Fig.11B, C, D).
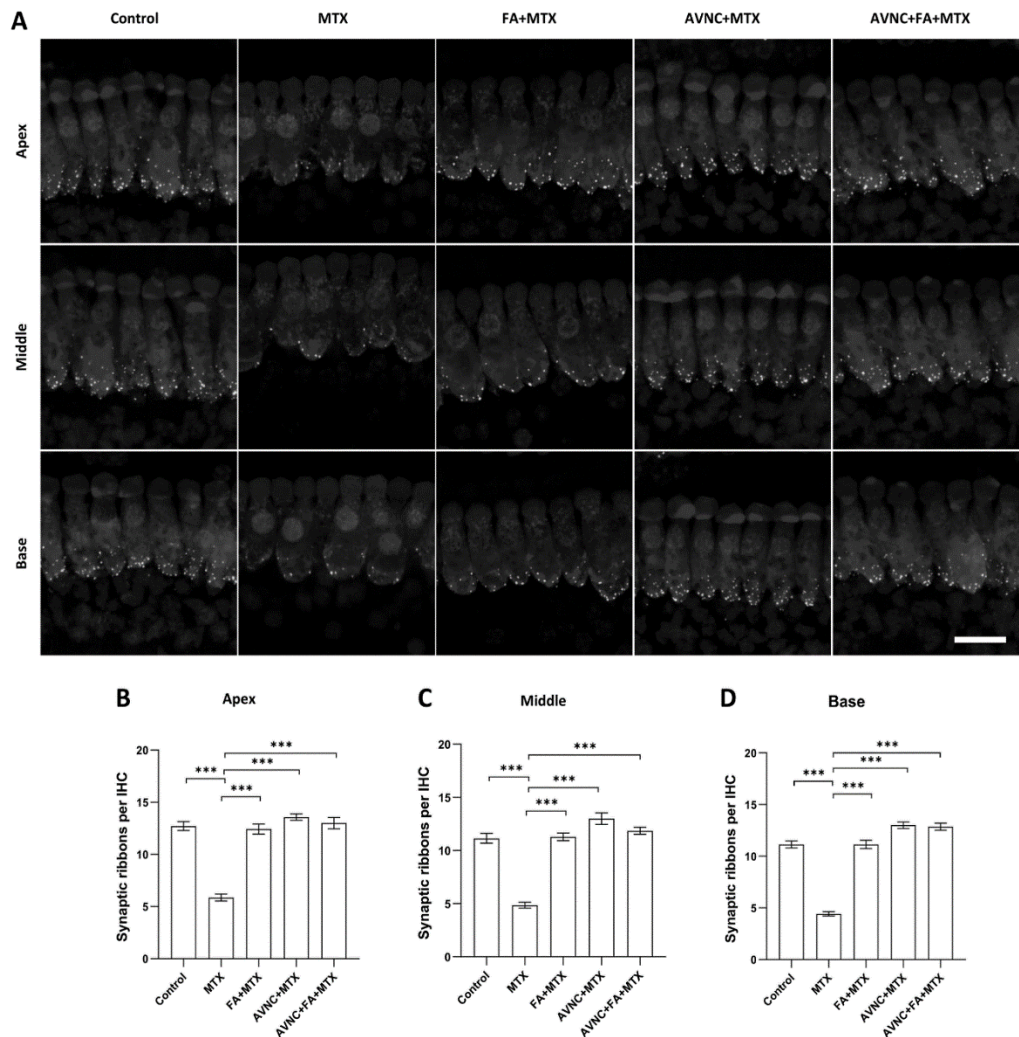
Figure 11. CtPB2 staining demonstrates that AVN-C protects cochlear synaptic damage incurred by MTX exposure. (A) MTX diminished synapses in all three regions of the cochlea. (B) and (C) and (D) Apex turn (21.7 ± 8.3), middle (18.7 ± 5.9), base (13.4 ± 2.6). (B) and (C) and (D) AVN-C protected cochlear synapses: apex turn (53.7 ± 4.9), middle (53.4 ± 2.4), base (52.3 ± 3.9). FA+MTX group (48.8 ± 5.3, 44.7 ± 6.8, and 44.1 ± 6.9, respectively), AVN-C+FA+MTX group (51.1 ± 6.3, 49.7 ± 6.9, 51.8 ± 6.8 respectively), and finally control group (49.1 ± 5.6, 43.3 ± 5.8, 44 ± 4, respectively). P-value ***$p < 0.001$. The white dots are synapses marked with CtBP2, whereas the inner hair cells are labeled with myosin-7a. Three mice were used for each group, and scale bar indicates 20 μm. Published data. Plos One DOI: 10.1371.

Furthermore, to measure the influence of MTX on hearing, we collected wave I at 90 dB SPL from each set of tested mice's saved ABR raw data using the R program (version 4.0.4). The amplitude of wave I was as follow: control (903.6 ± 10.3 nV), MTX (38.6 ± 6.2 nV), FA+MTX

(687.9 ± 10.8 nV), AVN-C+MTX (1,345.1 ± 13.7 nV) and AVN-C+FA+MTX (1,048.3 ± 10.7 nV) (Fig.11D).

4.6.   AVN-C inhibits the deterioration of spiral bundle axonal neurons.

We treated all cochleae with NF200 antibody and observed cochlear shape under a confocal microscope to check for cochlear atrophy along to the cochlea. In the MTX-treated population, cochlear neurodegeneration was more evident in the basal turn of the cochlea than in the middle and apex of the cochlea. The continuity and integrity of cochlear neurons in ascending position at the basal turn were destroyed in the FA+MTX-treated group, whereas those of neurons in the middle and apex turns were retained. Moreover, both the antioxidant AVN-C and the combining of AVN-C and FA resulted in the well neuronal health of the cochlea, whereas MTX exposure resulted in neuronal degeneration across the cochlear turns (Fig.12B).
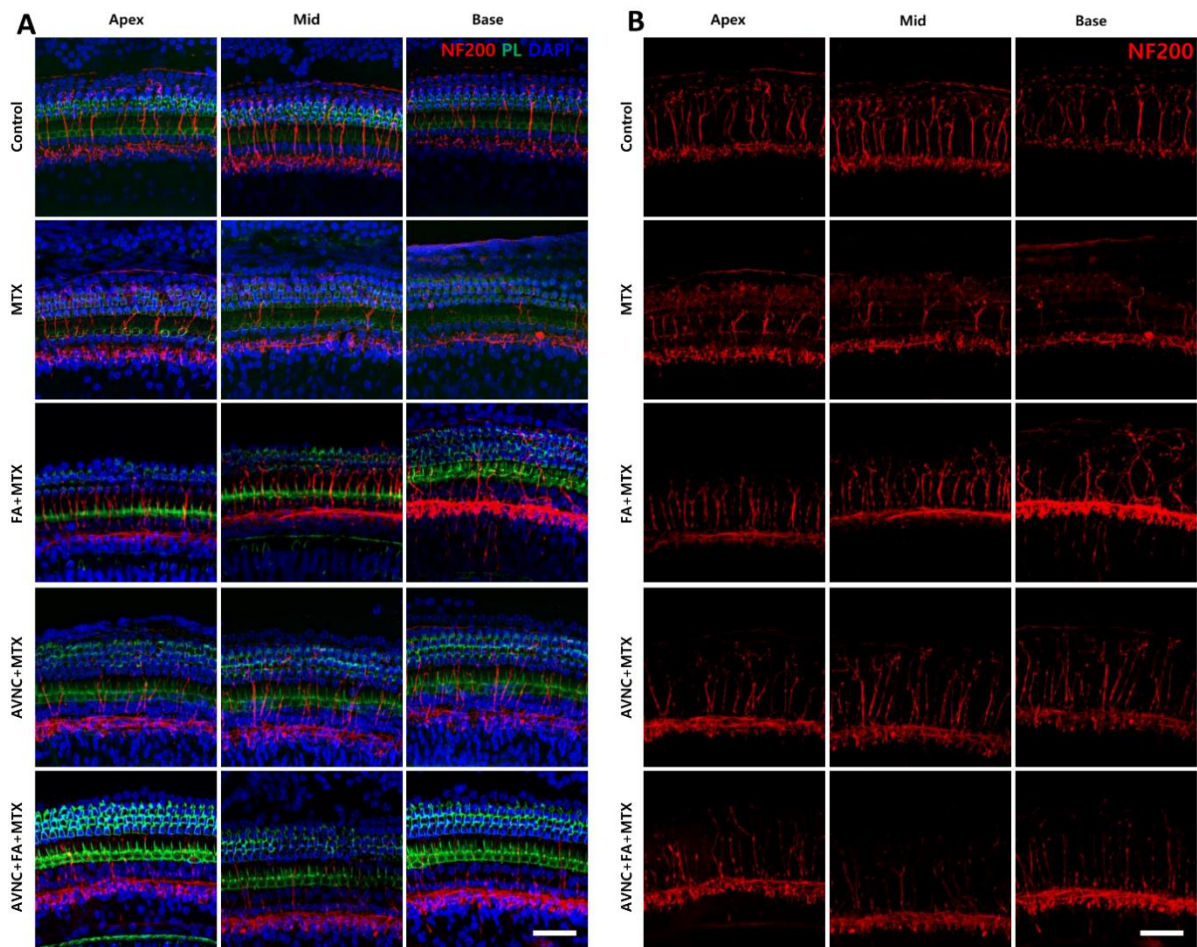
Figure 12. The cochlear neuron integrity is protected by AVN-C from the harmful effects of MTX. NF 200 was used to evaluate cochlear degeneration down to the cochlea. (A). A confocal microscope revealed substantial loss of cochlear nerves in the MTX group, which was more apparent at the basal turn than in the middle and apex regions. (B). The cochlear nerves at the basal turn displayed interruption in the upward position but were intact in the middle and apex turns of the cochlea in the FA+MTX. AVN-C alone or in conjunction with FA, led in well-defined cochlea neuronal health, whereas treatment with MTX caused the loss of neuron integrity across the cochlear turns. (A) and (B): NF200, Phalloidin (PL), and DAPI have been employed in staining; the combined picture depicts the OHCs. The scale bar indicates 50 µm. Published   data. Plos One DOI: 10.1371.

4.7. AVN-C protects cells against MTX and cisplatin-induced cytotoxicity.

The 3-(4,5-dimethylthiazol-2-yl)-2,5-diphenyltetrazolium bromide (MTT) assay, a colorimetric test that analyzes both metabolic cellular functions and the percentage of live cells remaining, was done on HEI-OC1 cells after treatment with AVN-C and/or FA and MTX; AVN-C and CP. The vitality of HEI-OC1 cells was determined in a quantitative and time dependent way. We first assessed the ratios of MTX (Fig.13A), AVN-C (Fig.13B), and CP (Fig.13D) in HEI-OC1 cells by assessing several dosing sequences before deciding on the right drug dose concentration to be employed. However, FA 3 μM was picked randomly and was used in either alone or in combination with AVN-C before MTX. In cisplatin and HEI-OC1 study, 30 μM was added to cells following AVN-C as described in the Figure 5. After completion of all treatment schedules and MTT assay, the absorbance of HEI-OC1 cells was measured at 570 nm with spectrophotometry. The cell growth was lowered by MTX 54.2 ± 13.3% (***$p < 0.001$), ending to cell death (Fig.13C). AVN-C raised the cells healthy to 88.3 ± 8.2% (***$p < 0.001$); AVN-C+FA cells viable was 86.3 ± 8.2% (***$p < 0.001$) and FA+MTX at 66.2 ± 13.1%. In cisplatin study, cisplatin caused death of many HEI-OC1 cells 51.8 ± 2.7 (Fig.13D) and AVN-C maintained many healthy cells at 81.2 ± 7.3 (Fig.13E).
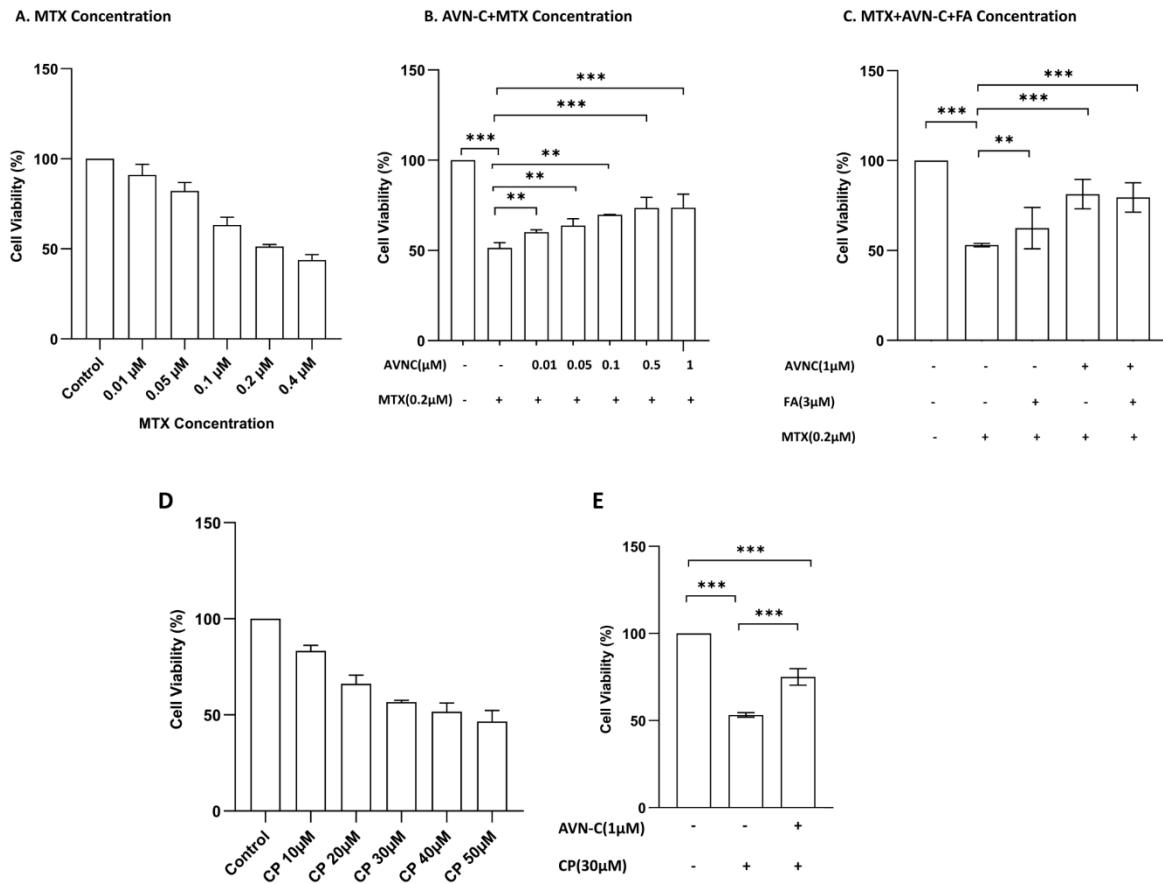
Figure 13. AVN-C, MTX and CP cell viability is dose-dependent. Figures A, B and C. Published data. Plos One DOI: 10.1371.

The cytotoxicity of MTX and CP in HEI-OC1 cells is dosage dependent. At concentration ≥ 0.2 μM for MTX, cell viability was diminished (Fig.13A); and for CP ≥ 30 μM 24 hours after treatment (Fig.13D). When the concentration of AVN-C was increased in cells treated with 0.2 μM of MTX, the viability of the cells increased (Fig.13B). The pretreatment of HEI-OC1 cells with 1 μM of AVN-C and 3 μM of FA for 3 hours before 0.2 μM of MTX for 24 hours, showed that AVN-C alone or AVN-C with FA possess a protective effect over MTX cytotoxicity and FA had moderate impact (Fig.13C). AVN-C decreased cisplatin-induced ototoxicity *in vitro* (Fig.13E). P-value *** $p < 0.001$, and the experiments were repeated differently three times.

4.8. In the *in vitro* HEI-OC1 investigations, AVN-C reduced ROS levels in MTX and cisplatin-induced ototoxicity

After finishing all dosing regimens to HEI-OC1 cells, the cells were incubated with cell-permeable 2,7-dichlorodihydrofluorescein diacetate (DCFDA) for thirty min at 37°C in 5% CO_2 and then analyzed for FACS analysis to assess ROS generation. The fluorescein-DCFDA channel positive group in HEI-OC1 cells treated with MTX alone and CP alone generated significantly greater ROS levels across both MTX (Fig.14A) and CP (Fig.14C) than all the other groups. The administration of AVN-C and/or FA three hours before MTX significantly reduced ROS (Fig.14 B). Similarly, when HEI-OC1 cells were administered AVN-C 3 hours earlier, CP cytotoxicity to HEI-OC1 cells was reduced (**p< 0.01; Fig.14D).
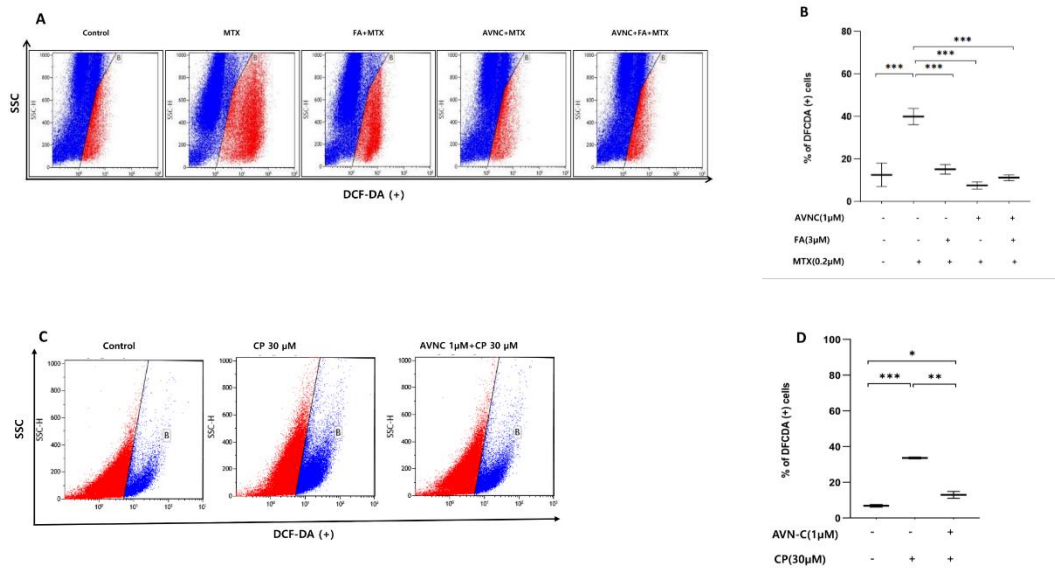
Figure 14. **ROS are reduced by AVN-C in MTX and cisplatin-induced ototoxicity in HEI-OC1 Cells**. Figures A and B. Published   data. Plos One DOI: 10.1371.

After removing the background, the acquired positive DCFDA percentages gated ROS. Flow cytometry and the DCFDA assay were used to measure the levels of intracellular ROS, and the

MTX or CP alone treated groups produced substantial amounts of ROS (Panel A and C). Pre - treatment with AVN-C and/or FA, on the other hand, lowered ROS levels both in MTX and CP (Panel B and D). Flow cytometry and the DCFDA assay were used to measure the levels of intracellular ROS, and the groups that only received MTX or CP produced a high amount of ROS (Panel A and C). Pretreatment with AVN-C and/or FA, on the other hand, lowered ROS levels in MTX and CP (Panel B and D).

4.9.   During an *in vitro* investigation, AVN-C inhibits the apoptotic signals of MTX and CP treatment.

Based on alterations in inflammatory cytokine expression patterns, RT-PCR was used to further unravel the downstream signaling pathways of AVN-C, FA, MTX, and CP. MTX increased the expression of all tested genes, including ROS and apoptotic genes (TNF, IL1, IL6, BAX, and HRK), and this was a consistent finding when the experiment was repeated. By lowering the cutoff expression levels of these genes, the addition of AVN-C or FA appeared to considerably reduce inflammation (Fig.15A, B, C, D, E). CP increased the level of inflammation related genes (TNF, IL1, iNOS, and COX2) on HEI-OC1 cells in the same patterns (Fig.15F, G, H, K). The experiment was conducted three times, and all comparison groups had a p-value of 0.05.
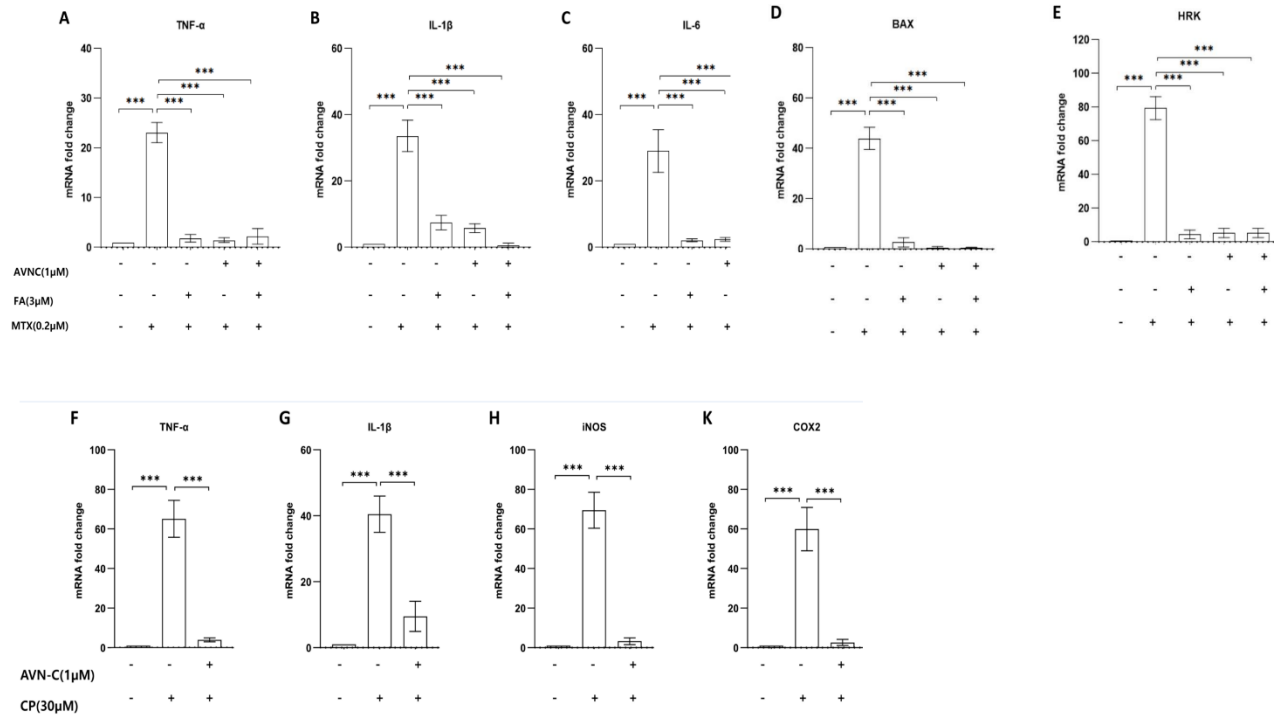
Figure 15. AVN-C and/or FA decrease apoptosis in HEI-OC1 cells of MTX, and Cisplatin-induced ototoxicity. Figures A, B, C, D and E. Published data. Plos One DOI: 10.1371.

The ototoxicity models of MTX and CP were developed in vitro on a HEI-OC1 cell. TNF-a, IL1b, and IL6 are major pro-inflammatory cytokines that play a role in the control of inflammatory reactions. The downstream genes of ROS and apoptosis were increased in the MTX-induced apoptosis group. In the MTX-treated group, BAX, a death-inducing member, and HRK, an apoptosis activator, are both considerably elevated. However, AVN-C and FA, either alone or in combination, dramatically normalized the expression of these genes in HEI-OC1 cells (***$p < 0.001$). In HEI-OC1 cells, CP enhanced inflammation related genes (Fig.15F, G, H, K). The experiments were repeated three times.

5. DISCUSSION

5.1. The AVN-C penetrated the blood labyrinth barrier.

In our prior study, we studied AVN-C in mouse blood serum after an intraperitoneal injection of 10 mg/kg of AVN-C and showed that AVN-C bioavailability peaked in the first hour after treatment and was washed out of the blood circulation within 6 hours. After delivering AVN-C to mice systemically, we looked for it in their perilymph. From the first hour to 3 hours after systemic injection, AVN-C was found in the perilymph, proving that it crosses the blood-labyrinth barrier and can work directly in the cochlea [14], and this was similar to what has been demonstrated by earlier works in human and rat [52, 53]. We noticed that AVN-C transited much longer in perilymph throughout our research, which explained its antioxidant impact in the cochlea, and that the half-life of molecules varied within the cochlea, which is consistent to earlier studies. Taken as examples, Dexamethasone-phosphate, rapidly depletes after 2–3 hours. Dexamethasone is kept in the body for more than 24 hours, and GM was somewhere in the middle [21].

5.2. DIHL and Oxidative Stress and Diseases

Some chemotherapy medications are known to be ototoxic agents, and more than a half million individuals in the globe develop cancer each year, with more than a quarter million dying from it. Instead of waiting for patients to complain before becoming concerned about hearing, oncologists' growing concern should lead to careful hearing loss prevention, including physical testing and careful monitoring of hearing losses; this means preventing the onset of hearing loss rather than only treatment when hearing can no longer be recovered [35, 58]. Platinum-

based anticancer drugs and aminoglycoside antibiotics were shown to be the most important in clinical practice among potentially ototoxic (harmful to the inner ear) treatments [59]. In a DIHL including Kanamycin and furosemide, the OHCs of all cochlea turns were extensively destroyed [14]. Normally, HD-MTX is quite often used in treating solid and haematological cancers, and some reports showed that it caused different side effects including neurological disturbance [60]. Furthermore, MTX caused hepato-renal injury [61] and intestinal damage [62] via oxidative stress and apoptosis in mice. However, there have been no DIHL studies that have investigated HD-MTX causing HL. Although, MTX-induced ototoxicity is not well studied, and many studies have reported the occurrence of MTX cytotoxicity to other normal organs; an important underlying mechanism was related to ROS production [63]. Hence, we evaluated the incidence of HD-MTX-induced ototoxicity and assessed the preventive role of antioxidant AVN-C for this condition.

5.3. Biodistribution/Pharmacodynamics of MTX following systemic administration - Plasma and inner ear

The quantity of MTX in the bloodstream initially peaked 30 minutes after it was administered to experimental mice but quickly declined until it was undetectable 8 hours later (Fig.6B) due to MTX uptake in the plasma, spleen, liver, gastrointestinal tract, kidney, muscles, skin, and bone marrow [64]. The serum concentrations of MTX in multidrug resistance protein 3 (MRP3 or ABCC3) knockout (KO) and wild-type (WT) mice were measured over time [65]. These mice were all given a single dosage of MTX (10, 50, or 200 mg/kg) through IV bolus. After 8 hours, the KO mice had significantly higher overall MTX clearance than the WT mice. This might account for its pharmacodynamics, absorption, and diffusion in a variety of tissues.

47

Furthermore, after administration, MTX is mainly dispersed to non-fatty body tissues, and it is quickly transferred across the blood capillaries and cell membrane of the liver, kidney, and skin, enabling tissue to plasma concentration equilibrium fractions to be formed on a time scale correlation with those of plasma flow restriction [64].

Similarly, we assessed the extent of MTX in the perilymph post systemic treatment to see if it had a direct negative effect on the cochlea. The emergence of MTX in the perilymph 1 hour after systemic injection verified the existence of MTX in the cochlea (Fig.6C). This could reflect MTX's direct deleterious effect on inner ear elements. A prior study [66] found that at therapeutic levels, MTX can cross the blood-brain barrier and reach the cerebrospinal fluid. Following an intravenous administration of this medication, the cerebrospinal fluid had less than 1 mM of MTX [67].

Similarly, a novel drug-fluorophore combination was created and tested as a tracer for determining cisplatin cellular uptake and in vivo distribution, and the uptake of CP by cochlear hair cells in the organ of Corti was then investigated. Outer hair cells (OHCs) showed modest fluorescence an hour after injection, especially on their stereocilia. At 1 hour after injection, inner hair cells (IHCs) did not fluoresce, but punctate fluorescence was detected in supporting cells surrounding IHCs, which was recognized as nonspecific autofluorescence as previously described. OHC and IHC stereocilia and cell bodies showed diffuse fluorescence from CP three hours after injection, and this fluorescence intensity was sustained 24 hours later [68]. These findings showed that CP passed the blood–labyrinth barrier (BLB) and infiltrated healthy rats' cochlear hair cells. Platinum-based chemotherapeutic agents routinely used in oncology (namely cisplatin, carboplatin, nedaplatin, and oxaliplatin) have diverse ototoxic and neurotoxic effects. When the BLB is disrupted by treatment with diuretics or noise exposure,

the uptake of drugs is increased and the extent of damage is greatly enhanced [69]. Our results indicate that MTX passes the BLB and directly destroys the OHCs, and earlier study has demonstrated that CP can pass the blood–labyrinth barrier and reach the cochlear hair cells of healthy rats.

5.4.   Counter Effect of MTX on Hearing (Low dose versus high dose)

A prospective open-label trial of 11 patients with treatment-refractory autoimmune hearing loss was carried out to evaluate the usefulness of minimal MTX as long-term care for autoimmune hearing loss. At the outset of this trial, at least one ear demonstrated an improvement in audiometric variables (Permanent Threshold (PT) by >10 dB or standard deviation (SD) by >15 percent). Long-term low-dose therapy of MTX has been shown to be successful in some patients with hearing loss suspected to be caused by autoimmunity and unresponsive to standard treatments [70]. Additional study found that intratympanic MTX administration has no ototoxic effects; this study indicated that this procedure can be properly performed and used as a suitable therapy option for autoimmune vestibulocochlear illnesses [71].

In our investigation, HD-MTX treatment caused DIHL with permanent threshold shifts—both in the click sound and in all evaluated frequencies of tone bursts—one month after treatment (Fig.7B, C). Low-dose MTX treatment, on the other hand, prevented the release of immune cells in animals with an autoimmune illness without having a major impact on the cochlea [70]. Generally, methotrexate dosages are classified into three groups clinically. Group one is called: "low-dose methotrexate" and is assigned to be as less than 20 mg/m^2 (LDMTX ≤ 0.66 mg/kg), and is commonly employed to treat rheumatological disorders like rheumatoid arthritis. Group

two comprises doses ranging from 100–500 mg/m^2 (3.3–16.6 mg/kg) and is classified as "intermediate" and are prescribed in case of solid tumors and breast tumors, even in case of lymphomas and low-grade leukemias. The last group stands for high-dose MTX, and is defined to be the dose greater than or equal to 500 mg/m^2 (HDMTX $\geq$16.6 mg/kg), and is mainly used as IV chemotherapy for high-grade leukemias/lymphomas such as non-Hodgkin lymphoma, osteosarcoma, and primary central nervous system lymphoma; and these treatment regimens are administered over several days [72]. This medication has the possibility to trigger treatment-related illness or death. As a result, it is vital to weigh the advantages and disadvantages.

5.5. AVN-C Forbids MTX-Induced Hearing Loss and Damage of Outer Hair Cells

Hearing loss can still have a huge impact on a patient's quality of life; thus ototoxicity should be taken into account during oncological therapy. One method of minimizing hearing loss is to diagnose ototoxicity to take prevention strategies. In our investigation, HD-MTX increased both click and tone burst sounds in wild type mice, leading in irreversible hearing loss (Fig. 7B, C). Furthermore, pre-treatment with AVN-C before to MTX treatment safeguarded the hearing of the wild type mice; these mice that received AVN-C replicated the outcomes of the control treated mice only the vehicle (Fig. 7B, C). Whenever the cochleae of all treated and non-treated (control) mice have all been planned for scanning electromicroscopy to probe greater depth into cochlea morphologies, we found a reduction in OHCs in the treated MTX group, but mice that received AVN-C and/or FA before MTX had a higher number of OHCs,

and the AVN-C only treated group surpassed other treatment timelines (Fig. 9A, B, C, D). Outer hair cells play a role in hearing that is linked to their motor function [73].

Despite the fact that HD-MTX is frequently used to treat blood malignancies, certain data indicate that it is connected with a variety of negative effects [60]. Furthermore, HD-MTX led to severe liver, renal, and gastrointestinal injury by apoptosis [62] and this might the same way it caused hearing loss during my experiment. However, by expanding our research into the positive protective effect of AVN-C on ototoxicity, we observed that AVN-C provided significant protection to the cochlea and hearing function. Moreover, folinic acid (FA) has also been widely studied and reported as an antidote to MTX, and it was used in this study to analyse the favourable protective impact of AVN-C. It has been used as an additive in all the HD-MTX experiments [74]. Furthermore, we hypothesized that this could explain why no hearing impairment was detected in mice treated with HD-MTX. Furthermore, the treatment of the antioxidant AVN-C reduced hearing problem related to oxidative stress in mice both NIHL and DIHL [14]. Nonetheless, combining AVN-C and FA treatment prior to HD-MTX delivery exhibited no further effects, indicating that AVN-C and FA share the same route. Since the antioxidant AVN-C protected against MTX toxicity, it is reasonable to believe that MTX ototoxicity included the formation of ROS.

5.6. AVN-C protects against hearing loss and outer hair cell loss brought on by cisplatin

Contrastingly, the relative ototoxicity of various platinum anticancer drugs, drug-dosing conditions that exacerbate ototoxicity, cochlear structures that are most vulnerable to platinum damage, therapies for reducing ototoxicity, and the molecular signaling pathways that lead to cell death in the inner ear have all been studied extensively over the last 30 years [70]. Even though they all have a platinum backbone, cisplatin may have quite diverse ototoxic effects from the rest of the group. Some of the differences are probably due to their chemical makeup. Individual patient characteristics also play a role, since a pharmacological dose that is ototoxic in one person may not be ototoxic in another.

In my experiments using B6 wild type mouse, CP caused irreversible hearing loss (Fig.8A, B) and a huge demise OHCs (Fig.10A, B, C) one month after IP treatment, but inner hair cells (IHCs) remained intact (Fig.10D). Moreover, AVN-C treated in advance to CP rescued hearing from cisplatin-induced ototoxicity and shielded OHCs from cisplatin harmful effect (Fig.10A, B, C). The mouse cochlea was subsequently dissected and stained to assess both the effect of AVN-C and CP on the OHCs, and our findings revealed that a large number of OHCs was lost in CP treated group, and it was more evident at the base, middle, and apex turns (Fig.10A, B, C), and even here AVN-C protected OHCs.

Furthermore, Cisplatin is known to destroy hair cells, with outer hair cells being more susceptible than inner hair cells [75, 76]. Reports revealed that Cisplatin-induced hearing loss is usually bilateral and starts at high frequencies before progressing to lower frequencies with

continued therapy [77, 78]. Symptoms frequently appear days or weeks after starting therapy and can continue to worsen even after treatment is stopped [79]. In-patients with certain risk factors may be an exception to this chronological progression. Hearing loss can occur quickly in this group of individuals, sometimes as a result of just one dose of the medicine [80]. Much research has focused on HL produced by cisplatin in the prevention of DIHL. Here, we cite alpha-lipoic acid [81], dunnione7 [82], R-phenylisopropyladenosine [83], Bucillamine [84], and Forskolin [85], have all been shown to protect against cisplatin ototoxicity in vivo animal trials and AVN-C enters in this range of protective agents against cisplatin-induced ototoxicity.

5.7.   Damage of Synapses and Neurons by MTX and Rescue by AVN-C/FA

Ribbon synapses connect the IHCs to the spiral ganglion neurons (SGNs), which are the primary synaptic structures in the sound conduction pathway and play a key role in sound signal transmission [86]. Damage to the ribbon synapses hinders transmission of sound and conduction to the brain (where it is interpreted as sound), thereby increasing the hearing thresholds and causing hearing loss. Additionally, MTX treatment impairs both the central and peripheral nervous systems, with the potential for neurotoxicity in the central auditory nervous system [29]. Our results showed a considerable decline in the number of ribbon synapses of IHCs in the MTX-treated group (Fig.11A, B, C, D). This finding suggests that HD-MTX has a direct harmful effect on the ribbon synapses. Meanwhile, AVN-C given in beforehand to MTX yielded enough protection to cochlear synapses either given alone or in concomitant to FA (Fig.11A, B, C, D).

Ribbon synapses are needed for phase locking and spatial sound localization in the mammalian auditory system [87]. They're vesicle-associated structures that play a role in synaptic vesicle

trafficking and fusion at presynaptic terminals [88]. Dendritic SGNs can be reduced by using NMDA glutamate receptor blockers like kynurenate and DNQX. MK-801, an antagonist for the NMDA subtype of glutamate receptors, for example, is beneficial against NIHL; however, it is unclear whether this protection is due to the preservation of synapses between IHCs and SGNs or other processes [89]. We demonstrate here that AVN-C is effective in protecting and preserving cochlear synapses from this chemotherapy agent MTX. However, the number of SGNs was maintained (data not shown).

Furthermore, MTX caused the death of several axons of the auditory nerve fibers, reduced the neural output of the cochlea, and impaired the sensitivity and optimization of auditory nerve fibers. Adding to these findings, wave I amplitude was significantly reduced, implying a decrease in the firing of electrical impulses from the cochlea to the brain for sound interpretation, eventually leading to hearing loss (Fig 7.D). However, AVN-C maintained the integrity of auditory nerve fibers better than FA, as I observed neuron discontinuity at the base turn of the cochlea in the group that was treated with FA and MTX.

In addition, the accumulation of ROS caused by cisplatin treatment and aging reduced the number of ribbon synapses in IHCs, resulting in synaptopathy and OHC loss, and suggested that ROS-induced impairment in the ribbon synapses is a precursor to hearing loss. In another previous study, the noise exposure resulted in significant reductions in ABR wave I amplitudes and loss of cochlear ribbon synapses in mice [90]. ABR amplitudes have been used successfully to alienate synaptopathy in listeners, considering that wave I depicts the synchronous firing of many auditory nerve fibers in the spiral ganglion cells [91].

The treatment methods used in our study (AVN-C, FA, and AVN-C+MTX) all offered protection towards HD-MTX toxicity, with AVN-C outperforming FA alone and AVN-C+FA

in respect of cochlear synapse and neuronal integrity preservation (Fig.11A.B, C, D and Fig.12A, B). Because AVN-C alters membrane fluidity and physical state [92], it improves integral membrane function by lowering endogenous ROS levels. Furthermore, AVN-C supplementation at a dose of 0.1 g/kg in the diet of rats was notably successful in decreasing the levels of ROS in the soleus muscle during *in vivo* studies and thus acted as a viable dietary antioxidant supplement [93], and all these results support the efficacy of AVN-C to preserve hearing from all harm of these chemotherapy drugs (MTX and CP).

Notwithstanding a considerable drop in ABR wave I amplitude data in the MTX group due to oxidative stress, AVN-C treatment significantly enhanced and maintained wave I amplitude, beating FA and the simultaneous AVN-C and FA treatment (Fig.7D). The drug regimens (AVN-C, FA, and AVN-C+FA) demonstrated the ability to protect and retain ribbon synapses (Fig.11B, C, D). This makes sense because AVN-C, as a potent antioxidant susceptible of lowering ROS levels, protected the ribbon synapses from the harmful effects of ROS.

Conversely, FA is commonly known as an antidote to MTX and was used in this experiment to treat MTX toxicity. Nevertheless, AVN-C was more efficient than FA in restoring cochlear nerve fiber axon quality; minor innervation deformity was seen at the basal turn in FA-treated cochlea (Fig.12B). After the damage caused by MTX, AVN-C appeared to promote cochlear neuron survival, which may have boosted the firing of electrical impulses from the cochlea to the brain, explaining the good ABR results when compared with those treated with MTX. Previously, it was demonstrated that the functional recovery of regenerated synapses in treated animals using round-window delivery of NT3 protein by evaluating the suprathreshold amplitude of ABR wave 1 in response to tone pips in the damaged cochlear frequency regions [94]. Based on the current widely accepted theory of mammalian cochlear mechanics, the fluid

in the cochlear scalae interacts with the elastic cochlear partition to produce transversely oscillating displacement waves that travel along the cochlear coil [95]. Furthermore, previous studies showed that exogenous neurotrophins directly delivered to the cochlear fluids enhance the survival of cochlear neurons after the hair cells are damaged by ototoxic drugs [96]. The contribution of antioxidant AVN-C was reported in all in vivo studies, as expected from our earlier work [14], and FA was found to block MTX ototoxicity.

5.8. In MTX and Cisplatin-induced ototoxicity in HEI-OC1 cells, AVN-C Reduces ROS

Drug-induced stress promotes ROS formation within the mitochondria of hair cells, which raises inflammatory levels, and the cascade finishes with hair cell apoptosis, resulting in hearing loss.

To better understand the role of ROS in the mechanism of MTX-induced apoptosis and the effects of AVN-C and FA, we pre-treated HEI-OC1 cells with 1 µM of AVN-C and 3 µM of FA for 3 hours before administering 0.2 µM of MTX. After 24 hours of MTX treatment, all the cells were examined under a fluorescence microscope.

Furthermore, DCF (a fluorescent probe commonly used to detect total ROS in cells) was used to measure the amount of ROS production. We observed that MTX-treated HEI-OC cells had a higher DCF-positive population, implying that MTX induces ROS generation (Fig.14A). After gating and retracting the background, the quantification of these ROS revealed an increase in ROS that was roughly two times that of the other groups (Fig.14B). When CP was applied to HEI-OC1 cells, the same results were obtained, and the formation of ROS was also

doubled (Fig.14C, D). Moreover, Huang et al. showed that MTX causes potent mitochondrial disruption and apoptosis in HL-60 and Jurkat T cells through the production of ROS [63]. Therefore, the role of MTX in mediating ROS production was dose dependent (data not shown). The apoptotic morphological changes were significantly reduced when the cells were pretreated with ROS scavenger AVN-C, and the antidote FA (Fig.14A, B). This antioxidant AVN-C showed to be a potent and powerful scavenger of ROS even in cisplatin-induced cytotoxicity (Fig.14C, D).

The mechanism of cisplatin-induced ROS formation and their contribution to cisplatin cytotoxicity in normal and cancer cells, however, is yet unknown. Using a panel of normal and cancer cell lines as well as the budding yeast Saccharomyces cerevisiae as a model system, researchers demonstrated that cisplatin causes a mitochondrial-dependent ROS response that amplifies the lethal effect of nDNA damage [97]. The quantity of cisplatin-induced nDNA damage had no effect on ROS formation, which happens in mitochondria as a result of protein synthesis impairment. Additionally, ROS are known to be extremely dangerous, triggering oxidative stress through the oxidation of biomolecules and resulting in irreversible cellular damage and cell death [98].

The inflammatory cytokines (TNF-α, IL1b, IL6, BAX, and HRK) were significantly upregulated in HEI-OC1 cells treated with MTX (Fig.15A, B, C, D, E, F). The overexpression of BAX in the MTX-treated cell group indicates that MTX induces ROS via a mitochondria-mediated pathway, leading to an increase in inflammation, thus apoptosis of inner ear structures. Despite using FA (a known antidote to MTX toxicity), either alone or in combination with AVN-C, the administration of antioxidant AVN-C alone was significantly effective at reducing ROS production and inflammation, preventing ototoxicity in HEI-OC1

cells. AVN-C has previously been shown to protect HEI-OC1 cells against gentamicin-induced oxidative damage [14].

In HEI-OC1 cells, AVN-C suppressed the inflammatory response induced by CP (Fig.15F, G, H, K), demonstrating a method to protect these cells against the ototoxicity of these two extensively used chemotherapeutic drugs (MTX and CP).

6. CONCLUSION

We firstly proved that MTX treatment results in substantial hearing loss. It can permeate the BLB in significant concentrations, causing injury to OHCs, cochlear neurons, and the ribbon synapses. The antioxidant AVN-C owns a significant protective effect on HD-MTX-induced ototoxicity, and we used FA in our studies to evaluate the efficacy of AVN-C. In MTX or CP-induced ototoxicity, AVN-C protects OHCs, ribbon synapses, cochlear neuron integrity, and improves ABR results. Avn C specifically inhibited inflammation by reducing inflammatory cytokines in HEI-OC1 cells. All of these suggests that AVN-C can be utilized to preserve hearing. Our findings suggest that AVN-C could be used to prevent HL during MTX or CP anti-cancer therapy.

7. REFERENCES

1. Robles, L. and M.A. Ruggero, *Mechanics of the mammalian cochlea.* Physiological Reviews, 2001. **81**(3): p. 1305-1352.
2. Betlejewski, S., *Science and Life--the history of Marquis Alfonso Corti.* Otolaryngologia polska= The Polish Otolaryngology, 2008. **62**(3): p. 344-347.
3. Fechner, F., et al., *Dense innervation of Deiters' and Hensen's cells persists after chronic deefferentation of guinea pig cochleas.* Journal of Comparative Neurology, 1998. **400**(3): p. 299-309.
4. Shokrian, M., et al., *Mechanically facilitated micro-fluid mixing in the organ of Corti.* Scientific Reports, 2020. **10**(1): p. 1-10.
5. Sterling, P. and G. Matthews, *Structure and function of ribbon synapses.* Trends in Neurosciences, 2005. **28**(1): p. 20-29.
6. Alpadi, K., et al., *RIBEYE recruits Munc119, a mammalian ortholog of the Caenorhabditis elegans protein unc119, to synaptic ribbons of photoreceptor synapses.* Journal of Biological Chemistry, 2008. **283**(39): p. 26461-26467.
7. Jean, P., et al., *The synaptic ribbon is critical for sound encoding at high rates and with temporal precision.* Elife, 2018. **7**: p. e29275.
8. Uthaiah, R.C. and A. Hudspeth, *Molecular anatomy of the hair cell's ribbon synapse.* Journal of Neuroscience, 2010. **30**(37): p. 12387-12399.
9. Moser, T. and C. Vogl, *New insights into cochlear sound encoding.* F1000Research, 2016. **5**.
10. Rutherford, M.A. and T. Moser, *The ribbon synapse between type I spiral ganglion neurons and inner hair cells*, in *The primary auditory neurons of the mammalian cochlea.* 2016, Springer. p. 117-156.
11. Furman, A.C., S.G. Kujawa, and M.C. Liberman, *Noise-induced cochlear neuropathy is selective for fibers with low spontaneous rates.* Journal of Neurophysiology, 2013. **110**(3): p. 577-586.
12. Han, B.I., et al., *Tinnitus: characteristics, causes, mechanisms, and treatments.* Journal of Clinical Neurology, 2009. **5**(1): p. 11-19.
13. Handzel, O., B.J. Burgess, and J.B. Nadol Jr, *Histopathology of the peripheral vestibular system after cochlear implantation in the human.* Otology & Neurotology, 2006. **27**(1): p. 57-64.
14. Umugire, A., et al., *Avenanthramide-C prevents noise-and drug-induced hearing loss while protecting auditory hair cells from oxidative stress.* Cell Death Discovery, 2019. **5**(1): p. 1-11.
15. Wang, Y., K. Hirose, and M.C. Liberman, *Dynamics of noise-induced cellular injury and repair in the mouse cochlea.* Journal of the Association for Research in Otolaryngology, 2002. **3**(3): p. 248-268.
16. Rutherford, M.A. and T. Moser, *The ribbon synapse between type I spiral ganglion neurons and inner hair cells*, in *The primary auditory neurons of the mammalian cochlea.* 2016, Springer. p. 117-156.
17. Wan, G. and G. Corfas, *Transient auditory nerve demyelination as a new mechanism for hidden hearing loss.* Nature Communications, 2017. **8**(1): p. 1-13.
18. Scholz, J. and C.J. Woolf, *The neuropathic pain triad: neurons, immune cells and glia.* Nature Neuroscience, 2007. **10**(11): p. 1361-1368.
19. Themann, C.L. and E.A. Masterson, *Occupational noise exposure: A review of its effects, epidemiology, and impact with recommendations for reducing its burden.* The Journal of the Acoustical Society of America, 2019. **146**(5): p. 3879-3905.
20. Kujawa, S.G. and M.C. Liberman, *Adding insult to injury: cochlear nerve degeneration after "temporary" noise-induced hearing loss.* Journal of Neuroscience, 2009. **29**(45): p. 14077-14085.

21. Vara, D. and G. Pula, *Reactive oxygen species: physiological roles in the regulation of vascular cells.* Current Molecular Medicine, 2014. **14**(9): p. 1103-1125.

22. Gorelick, P.B., et al., *Vascular contributions to cognitive impairment and dementia: a statement for healthcare professionals from the American Heart Association/American Stroke Association.* Stroke, 2011. **42**(9): p. 2672-2713.

23. Kehrer, J.P., *Free radicals as mediators of tissue injury and disease.* Critical Reviews in Toxicology, 1993. **23**(1): p. 21-48.

24. Bergamini, C.M., et al., *Oxygen, reactive oxygen species and tissue damage.* Current Pharmaceutical Design, 2004. **10**(14): p. 1611-1626.

25. Howard, S.C., et al., *Preventing and managing toxicities of high-dose methotrexate.* The Oncologist, 2016. **21**(12): p. 1471.

26. Vincenzi, B., et al., *Drug-induced hepatotoxicity in cancer patients-implication for treatment.* Expert Opinion on Drug Safety, 2016. **15**(9): p. 1219-1238.

27. Youssef, A.A., T.A. Raafat, and Y. Madney, *Child with acute methotrexate related neurotoxicity: Can diffusion weighted MRI help??* The Egyptian Journal of Radiology and Nuclear Medicine, 2015. **46**(4): p. 1149-1153.

28. Ziereisen, F., et al., *Reversible acute methotrexate leukoencephalopathy: atypical brain MR imaging features.* Pediatric Radiology, 2006. **36**(3): p. 205-212.

29. Leite, R.A., et al., *Brainstem auditory pathway of children with acute lymphoid leukemia on chemotherapy with methotrexate.* Arquivos de Neuro-psiquiatria, 2020. **78**(2): p. 63-69.

30. Umugire, A., et al., *Efficiency of antioxidant Avenanthramide-C on high-dose methotrexate-induced ototoxicity in mice.* Plos One, 2022. **17**(3): p. e0266108.

31. Hsu, C.-H., et al., *Combination chemotherapy of cisplatin, methotrexate, vinblastine, and high-dose tamoxifen for transitional cell carcinoma.* Anticancer Research, 2001. **21**(1B): p. 711-715.

32. Brace, K.M., et al., *Childhood leukemia survivors exhibit deficiencies in sensory and cognitive processes, as reflected by event-related brain potentials after completion of curative chemotherapy: a preliminary investigation.* Journal of Clinical and Experimental Neuropsychology, 2019. **41**(8): p. 814-831.

33. Go, R.S. and A.A. Adjei, *Review of the comparative pharmacology and clinical activity of cisplatin and carboplatin.* Journal of Clinical Oncology, 1999. **17**(1): p. 409-409.

34. Alchin, K.F., *Ototoxicity in patients receiving concurrent cisplatin and cranial irradiation therapy for the treatment of head and neck cancers: An Audiometric Follow-up.* 2010.

35. Bass, J.K., et al., *Evaluation and management of hearing loss in survivors of childhood and adolescent cancers: a report from the children's oncology group.* Pediatric Blood & Cancer, 2016. **63**(7): p. 1152-1162.

36. Laurell, G. and U. Jungnelius, *High-Dose cisplatin treatment: Hearing loss and plasma concentrations.* The Laryngoscope, 1990. **100**(7): p. 724-734.

37. Fernandez, K.A., et al., *Atorvastatin is associated with reduced cisplatin-induced hearing loss.* The Journal of clinical investigation, 2021. **131**(1).

38. Yadav, A., et al., *Antioxidants and its functions in human body-A Review.* Research in Environment and Life Sciences, 2016. **9**(11): p. 1328-1331.

39. Wichansawakun, S. and H.S. Buttar, *Antioxidant diets and functional foods promote healthy aging and longevity through diverse mechanisms of action*, in *The role of functional food security in global health*. 2019, Elsevier. p. 541-563.

40. Durazzo, A., et al., *Polyphenols: A concise overview on the chemistry, occurrence, and human health.* Phytotherapy Research, 2019. **33**(9): p. 2221-2243.

41. Alfieri, M. and R. Redaelli, *Oat phenolic content and total antioxidant capacity during grain development.* Journal of Cereal Science, 2015. **65**: p. 39-42.

42. Chmelová, D., et al., *Antioxidant activity in naked and hulled oat (Avena sativa L.) varieties.* Journal of Microbiology, Biotechnology and Food Sciences, 2021. **2021**: p. 63-65.

43. Martinez-Villaluenga, C. and E. Penas, *Health benefits of oat: Current evidence and molecular mechanisms.* Current Opinion in Food Science, 2017. **14**: p. 26-31.

44. Ryan, L., P.S. Thondre, and C.J.K. Henry, *Oat-based breakfast cereals are a rich source of polyphenols and high in antioxidant potential.* Journal of Food Composition and Analysis, 2011. **24**(7): p. 929-934.

45. Rasane, P., et al., *Nutritional advantages of oats and opportunities for its processing as value added foods-a review.* Journal of Food Science and Technology, 2015. **52**(2): p. 662-675.

46. Webster, F., *Oats: chemistry and technology.* 2016: Academic Press.

47. Zwer, P., *Oats: characteristics and quality requirements*, in *Cereal Grains*. 2010, Elsevier. p. 163-182.

48. Clemens, R. and B.J.-W. van Klinken, *The future of oats in the food and health continuum.* British Journal of Nutrition, 2014. **112**(S2): p. S75-S79.

49. Gilissen, L.J., I.M. Van der Meer, and M.J. Smulders, *Why oats are safe and healthy for celiac disease patients.* Medical Sciences, 2016. **4**(4): p. 21.

50. Daou, C. and H. Zhang, *Oat beta-glucan: its role in health promotion and prevention of diseases.* Comprehensive Reviews in Food Science and Food Safety, 2012. **11**(4): p. 355-365.

51. Dimberg, L.H., et al., *Stability of oat avenanthramides.* Cereal Chemistry, 2001. **78**(3): p. 278-281.

52. Koenig, R.T., et al., *Avenanthramides are bioavailable and accumulate in hepatic, cardiac, and skeletal muscle tissue following oral gavage in rats.* Journal of Agricultural and Food Chemistry, 2011. **59**(12): p. 6438-6443.

53. Chen, C.-Y.O., et al., *Avenanthramides are bioavailable and have antioxidant activity in humans after acute consumption of an enriched mixture from oats.* The Journal of Nutrition, 2007. **137**(6): p. 1375-1382.

54. Watson, R.R., V.R. Preedy, and S. Zibadi, *Polyphenols: prevention and treatment of human disease.* 2018: Academic Press.

55. Buran, B.N., et al., *Optimizing auditory brainstem response acquisition using interleaved frequencies.* Journal of the Association for Research in Otolaryngology, 2020. **21**(3): p. 225-242.

56. Colmenárez-Raga, A.C., et al., *Reversible functional changes evoked by anodal epidural direct current electrical stimulation of the rat auditory cortex.* Frontiers in Neuroscience, 2019. **13**: p. 356.

57. Llufrio, E.M., et al., *Sorting cells alters their redox state and cellular metabolome.* Redox Biology, 2018. **16**: p. 381-387.

58. Schultz, C., et al., *Report on hearing loss in oncology.* Brazilian Journal of Otorhinolaryngology, 2009. **75**: p. 634-641.

59. Schacht, J., A.E. Talaska, and L.P. Rybak, *Cisplatin and aminoglycoside antibiotics: hearing loss and its prevention.* The Anatomical Record: Advances in Integrative Anatomy and Evolutionary Biology, 2012. **295**(11): p. 1837-1850.

60. Jaffe, N., et al., *Transient neurologic disturbances induced by high-dose methotrexate treatment.* Cancer, 1985. **56**(6): p. 1356-1360.

61. Abdel-Daim, M.M., et al., *Diosmin attenuates methotrexate-induced hepatic, renal, and cardiac injury: a biochemical and histopathological study in mice.* Oxidative Medicine and Cellular Longevity, 2017. **2017**.

62. Aldhahrani, A., *Protective effects of guarana (Paullinia cupana) against methotrexate-induced intestinal damage in mice.* Food Science & Nutrition, 2021.

63. Huang, C., et al., *Ornithine decarboxylase prevents methotrexate-induced apoptosis by reducing intracellular reactive oxygen species production.* Apoptosis, 2005. **10**(4): p. 895-907.

64. Morrison, P.F., R.L. Dedrick, and R.J. Lutz, *Methotrexate: Pharmacokinetics and assessment of toxicity.* Drinking Water and Health, 1987. **8**.

65. Osman, A.-M.M., et al., *Pharmacokinetic profile of methotrexate and 5-fluorouracil in normal and bilharzial-infested mice.* Chemotherapy, 1994. **40**(4): p. 227-231.

66. Csordas, K., et al., *Comparison of pharmacokinetics and toxicity after high-dose methotrexate treatments in children with acute lymphoblastic leukemia.* Anti-Cancer Drugs, 2013. **24**(2): p. 189-197.

67. Yoshikawa, N., et al., *Measurement of methotrexate in human cerebrospinal fluid using a chemiluminescence immunoassay intended for serum and plasma matrices.* Journal of Clinical Laboratory Analysis, 2021. **35**(3): p. e23661.

68. Chu, Y.-H., et al., *Systemic delivery and biodistribution of cisplatin in vivo.* Molecular Pharmaceutics, 2016. **13**(8): p. 2677-2682.

69. Ding, D., B.L. Allman, and R. Salvi, *Ototoxic characteristics of platinum antitumor drugs.* The Anatomical Record: Advances in Integrative Anatomy and Evolutionary Biology, 2012. **295**(11): p. 1851-1867.

70. Matteson, E.L., et al., *Use of methotrexate for autoimmune hearing loss.* Annals of Otology, Rhinology & Laryngology, 2000. **109**(8): p. 710-714.

71. Eren, S.B., et al., *Evaluation of ototoxicity of intratympanic administration of Methotrexate in rats.* International Journal of Pediatric Otorhinolaryngology, 2017. **100**: p. 132-136.

72. LaCasce, A.S., *Therapeutic use and toxicity of high-dose methotrexate.* UpToDate. Waltham, 2014.

73. Bavi, N., et al., *The conformational cycle of prestin underlies outer-hair cell electromotility.* Nature, 2021. **600**(7889): p. 553-558.

74. Holmboe, L., et al., *High dose methotrexate chemotherapy: pharmacokinetics, folate and toxicity in osteosarcoma patients.* British Journal of Clinical Pharmacology, 2012. **73**(1): p. 106-114.

75. Takeno, S., et al., *Induction of selective inner hair cell damage by carboplatin.* Scanning Microscopy, 1994. **8**(1): p. 10.

76. Li, Y., et al., *Co-administration of cisplatin and furosemide causes rapid and massive loss of cochlear hair cells in mice.* Neurotoxicity Research, 2011. **20**(4): p. 307-319.

77. Callejo, A., et al., *Cisplatin-induced ototoxicity: effects, mechanisms and protection strategies.* Toxics, 2015. **3**(3): p. 268-293.

78. Galluzzi, L., et al., *Molecular mechanisms of cisplatin resistance.* Oncogene, 2012. **31**(15): p. 1869-1883.

79. Quasthoff, S. and H.P. Hartung, *Chemotherapy-induced peripheral neuropathy.* Journal of Neurology, 2002. **249**(1): p. 9-17.

80. Association, A.S.-L.-H., *Audiologic management of individuals receiving cochleotoxic drug therapy.* 1994.

81. Kim, K.-H., et al., *Evaluating protective and therapeutic effects of alpha-lipoic acid on cisplatin-induced ototoxicity.* Cell Death & Disease, 2018. **9**(8): p. 1-13.

82. Kim, H.-J., et al., *Dunnione ameliorates cisplatin ototoxicity through modulation of NAD+ metabolism.* Hearing Research, 2016. **333**: p. 235-246.

83. Kaur, T., et al., *Adenosine A1 receptor protects against cisplatin ototoxicity by suppressing the NOX3/STAT1 inflammatory pathway in the cochlea.* Journal of Neuroscience, 2016. **36**(14): p. 3962-3977.

84. Kim, S.-J., et al., *Bucillamine prevents cisplatin-induced ototoxicity through induction of glutathione and antioxidant genes.* Experimental & Molecular Medicine, 2015. **47**(2): p. e142-e142.

85. Guo, X., et al., *Forskolin protects against cisplatin-induced ototoxicity by inhibiting apoptosis and ROS production.* Biomedicine & Pharmacotherapy, 2018. **99**: p. 530-536.

86. Matthews, G. and P. Fuchs, *The diverse roles of ribbon synapses in sensory neurotransmission.* Nature Reviews Neuroscience, 2010. **11**(12): p. 812-822.

87. Palmer, A. and I. Russell, *Phase-locking in the cochlear nerve of the guinea-pig and its relation to the receptor potential of inner hair-cells.* Hearing Research, 1986. **24**(1): p. 1-15.

88. Snellman, J., et al., *Acute destruction of the synaptic ribbon reveals a role for the ribbon in vesicle priming.* Nature Neuroscience, 2011. **14**(9): p. 1135-1141.

89. Han, S., et al., *Nicotinamide riboside protects noise-induced hearing loss by recovering the hair cell ribbon synapses.* Neuroscience Letters, 2020. **725**: p. 134910.

90. Sheppard, A., et al., *Review of salicylate-induced hearing loss, neurotoxicity, tinnitus and neuropathophysiology.* Acta Otorhinolaryngologica Italica, 2014. **34**(2): p. 79.

91. Verhulst, S., et al., *Individual differences in auditory brainstem response wave characteristics: relations to different aspects of peripheral hearing loss.* Trends in Hearing, 2016. **20**: p. 2331216516672186.

92. Eze, M., *Membrane fluidity, reactive oxygen species, and cell-mediated immunity: implications in nutrition and disease.* Medical hypotheses, 1992. **37**(4): p. 220-224.

93. Monti, D.M., et al., *Role of antioxidants in the protection from aging-related diseases.* 2019, Hindawi.

94. Suzuki, J., G. Corfas, and M.C. Liberman, *Round-window delivery of neurotrophin 3 regenerates cochlear synapses after acoustic overexposure.* Scientific Reports, 2016. **6**(1): p. 1-11.

95. Nam, J.-H., *Microstructures in the organ of Corti help outer hair cells form traveling waves along the cochlear coil.* Biophysical journal, 2014. **106**(11): p. 2426-2433.

96. Richardson, R.T., F. Noushi, and S. O'Leary, *Inner ear therapy for neural preservation.* Audiology and Neurotology, 2006. **11**(6): p. 343-356.

97. Florea, A.-M. and D. Büsselberg, *Cisplatin as an anti-tumor drug: cellular mechanisms of activity, drug resistance and induced side effects.* Cancers, 2011. **3**(1): p. 1351-1371.

98. Marullo, R., et al., *Cisplatin induces a mitochondrial-ROS response that contributes to cytotoxicity depending on mitochondrial redox status and bioenergetic functions.* PloS One, 2013. **8**(11): p. e81162.

8. ACKNOWLEDGEMENT

9. 국문 초록

Avenanthramide-C Rescues Ototoxicity Induced by: Methotrexate or Cisplatin

Methotrexate 또는 Cisplatin 항암제 이독성에 대한 Avenanthramide-C의 보호 효과

서론 : 메토트렉세이트 (Methotrexate; MTX) 및 시스플라틴 (Cisplatin; CP)과 같은 항암 화학 요법 약물은 다양한 유형의 암을 치료하는 데 효과적이다. 그러나, 이들은 정상적인 기관과 세포들도 손상시킬 수 있다. 강력한 항산화제인 Avenanthramide-C (AVN-C)는 다양한 독성에 대해 세포들을 보호한다고 알려져 있다. 현재까지 MTX에 의해 유발된 청력 손실은 잘 알려지지 않았기 때문에 본 연구에서는 MTX가 청력에 미치는 영향을 조사하고 이와 관련된 메커니즘을 확인하고자 하였다. 또한, MTX와 CP에 의해 유발된 이독성에 대한 AVN-C 의 보호 효과를 증명하고자 하였다.

재료 및 방법: 정상 성체 C57BI/6 마우스를 이용하여 실험을 진행하였다. MTX의 혈청 및 외림프 농도는 액체크로마토그래피 질량 분석기를 사용하여 평가하였다. 메토트렉세이트 이독성 연구에서 5개의 연구 그룹 (대조군, MTX 군, MTX+folinc acid (FA) 군, MTX + AVN-C군, MTX + FA +AVN-C군)을 대상으로 청성뇌간유발 반응을 이용한 청력검사, 와우 시냅스, 청성뇌간유발 반응 검사에서의 I 파의 진폭 및 신경 손상 정도를 평가하였다. 이독성의 조직학적 검사을 위하여 외유모세포(Outer Hair Cells; OHCs)를 주사 전자현미경을 통하여 확인하였다. 또한, CP로 유도된 이독성에 대한 AVN-C 효능을 조사하기 위하여 각각 청성뇌간유발 반응검사를 통한 청력검사와 면역형광 염색을 통한 조직학적 검사를 시행하였다. In vitro 연구에서는 HEI-OC1 세포를 사용하여 각각의 군에 대하여 세포 사멸 여부를 확인하였고, RT-PCR을 이용하여 다양한 염증 및 활성산소 손상과 관련된 인자들 (TNFa, IL1b, IL6, BAX, HRK, iNOS 및

COx2)을 측정하였다.

결과: 메토트렉세이트 투여 30분 후에 혈청 및 외림프의 MTX 농도의 증가를 확인하였다. 고농도 MTX를 투여한 군에서 청력역치의 상승을 확인하였고, AVN-C 및 FA를 함께 투여시 청력역치 상승을 억제하였다. MTX 투여는 청성뇌간유발 반응검사에서 I 파의 진폭을 감소시켰으며, FA와 AVN-C는 이를 보존하였다. HEI-OC1 세포에 MTX를 투여시 세포 생존력을 감소 시켰고, 활성산소 (reactive oxygen species; ROS)의 농도를 증가시킨 반면, AVN-C 및 FA를 함께 투여시 ROS 발현을 억제하였다. 시스플라틴 유발 이독성 실험에서 AVN-C는 청력 역치 상승을 억제하고, 세포 생존력을 유지하였으며, CP 유발 이독성에서 OHC를 보호하였다. MTX 및 CP을 처리한 HEI-OC1 세포에서 염증과 관련된 인자들이 유의하게 상승하였고, AVN-C 및 FA 를 함께 투여시 이를 억제하였다.

결론: 고농도 MTX를 투여시 심각한 청력 손상을 유발하였으며, 이는 MTX가 혈액 미로 장벽을 투과하여 달팽이관내의 신경과 OHC의 손상을 야기함으로 발생하였다. 또한, 항산화제인 AVN-C는 항암제인 MTX 및 CP 유발 이독성에 대해 강력한 보호 효과를 발휘하였으며, 이는 MTX나 CP 에 의해 활성산소 발현증가로 이독성이 나타나며, AVN-C가 이 약물에 의한 활성산소 발현을 억제하여 청력의 보호효과를 나타낸다.